HDAC6 Inhibitors Sensitize Claudin-high Breast Cancer Cells to Cysteine Depletion via Activation of PKCγ Signaling

Tahiyat Alothaim
Michigan Tech: Michigan Technological University
Morgan Charbonneau
Michigan Tech: Michigan Technological University
Xiaohu Tang (xiaohut@mtu.edu)
Michigan Tech: Michigan Technological University https://orcid.org/0000-0001-6367-4991

Research article

Keywords: Cysteine dependence, synthetic lethality, claudin, zinc, biomarker

Posted Date: December 1st, 2020

DOI: https://doi.org/10.21203/rs.3.rs-116022/v1

Abstract

Introduction

Triple-negative breast cancer (TNBC) is a highly malignant breast cancer type with poor prognosis and lacks effective therapy. TNBC is not responsive to targeted therapy for hormone receptors and often exhibit resistance to current chemotherapeutic agents. Targeting tumor metabolism is an emergent strategy to treat cancer. Therefore, identification of tumor metabolic deregulations and development of effective targeted therapies are urgently needed.

Methods

We performed the epigenetic compound library screening in claudin-high breast tumor cells and identified therapeutical sensitizers to overcome the drug resistance of targeted cysteine-dependence therapy. Gene expression profiling were generated to analyze signaling pathways induced by the combined tubacin and cysteine deprivation treatment. Specific inhibitors, shRNA, and CRISPR/Cas9 gene editing approaches were used to target cellular proteins HDAC6 and PKCγ and examine their roles in cell death. Cell viability, RT-qPCR, and Western blotting assays were performed in cysteine-independent tumor cells to examine the anticancer effects of combined tubacin and cysteine deprivation treatment.

Results

We found that TNBC has differential death responses to cysteine deprivation and the cysteine-dependence of TNBC corelates with the expression levels of claudin genes in addition to the classical EMT markers. To overcome drug resistance in claudin-high/cysteine-independent breast tumor cells, HDAC6 inhibitors were identified by the epigenetic compound library screening as potent sensitizers that synergize with cysteine deprivation to eradicate cysteine-independent tumor cells. Unexpectedly, HDAC6 knockout did not recapitulate the HDAC6 inhibitors-mediated synthetic lethality, indicating that HDAC6 is not the actual target of HDAC6 inhibitors in this context. Transcriptomic profiling revealed that HDAC6 inhibitors synergizes with cysteine depletion to trigger a profound gene transcriptional program. Notably, a zinc-related gene response was observed to accompany with a prominent increase of labile zinc in cells during cell death. We further showed that activation of PKCγ signaling is required to interfere cellular zinc homeostasis and drive HDAC6 inhibitors-mediated cell death.

Conclusion

Our study demonstrated that HDAC6 inhibitors function as potent sensitizers to overcome the resistance of cysteine deprivation in claudin-high breast tumor cells. Identification of such sensitizers would make the targeted cysteine-dependence therapy applicable in various subtypes of breast cancer.

Background

Triple-negative breast cancer (TNBC) accounts for 15% ~ 20% of overall breast cancer cases and exhibits earlier age of onset, high metastasis, and aggressiveness with poor clinical outcomes shown by higher relapse and lower survival rates than other types of breast cancer [1–3]. TNBC contributes to the major mortality of breast cancer patients [4–6]. However, there is few clinically effective and targeted therapy for TNBC [7–9]. Treatments of TNBC patients are still limited to surgery, chemotherapy, or radiation since the absence of cell receptors makes targeted hormonal therapies impossible. About 50% of TNBC respond to conventional therapies, but the efficiency of treatments is limited by tumor metastasis and drug resistance [10, 11]. Therefore, there remains an urgent need to develop novel therapeutic approaches to improve cancer outcomes and reduce patient mortality.

With omics technologies, researchers have gained a deep understanding of molecular complexity of cancer [1, 12, 13]. Metabolic deregulation is an emergent hallmark in many cancers [14, 15]. Cellular metabolic rewiring often occurs with oncogenic alterations and microenvironmental adaptations to meet the demands of tumor cell survival, proliferation, and invasion [16–18]. For example, tumor cells acquire aerobic glycolysis (the Warburg effect) and redirect glucose metabolites into the pentose phosphate shunt pathway to maintain cellular redox and supply extra needs of nucleotides. Hence, these tumor cells are addicted to glucose and sensitive to inhibition of glycolysis by glucose analogues [19, 20]. Similarly, alteration of amino acid metabolism has been observed in many cancers associating with genetic aberrations. Oncogenic *MYC* activates glutaminolysis and establishes an alternative citric acid cycle to meet the demands of lipid biomass for fast cell proliferation, and *MYC*-induced tumors typically addict to glutamine [21, 22]. Overall, targeting metabolic vulnerabilities has been suggested as a promising targeted strategy to treat cancers.

Cysteine dependence/addiction as a metabolic vulnerability has been observed in many cancers [23–25]. The cysteine, mostly derived from extracellular disulfide cystine, is involved in cellular glutathione (GSH) synthesis that removes cytotoxic ROS and reactive nitrogen through the action of glutathione peroxidases (GPXs) [26]. Cystine deprivation or blocking the cystine/glutamate antiporter (the system xC-) by erastin or sulfasalazine limits the synthesis of cellular GSH, which leads to accumulation of lipid peroxidation, oxidative damage, and ultimately ferroptosis [23]. Ferroptosis is a new form of regulated and iron-dependent cell death, which is mechanistically distinct from necroptosis, autophagy, and other forms of non-apoptotic cell death and mostly induced by lethal lipid peroxidation [27, 28]. Targeting cysteine dependence/addiction could be an effective targeted cancer therapy since limiting single amino acid is relatively feasible and applicable to be achieved *in vivo* [29, 30]. Recently, a human-engineered enzyme “cysteinase” has been developed to deplete serum cystine/cysteine to suppress tumor growth in mice with a safe and effective efficacy [31, 32]. Cysteine dependence has been observed as a striking feature in TNBC [33]. However, only a subset of TNBC cells shows great sensitivity to cysteine depletion and the system xC- inhibitors. Little is known what mechanisms control the high-demand of cysteine in TNBC. Also, biomarkers are needed to identify to precisely determine the cysteine dependence in TNBC.

Epigenetic alterations including histone modifications and DNA methylation have been suggested to direct cancer development and progression [34]. Distinct DNA methylation patterns have been observed

to associate with luminal and basal subtypes of breast cancers when analyzing the omics of 802 breast tumor cases [35]. A high degree of DNA methylation deposits in aggressive metastatic breast cancer cells and a relative low level of histone acetylation and methylation associates with low prognostic breast cancers [35–38]. These suggest that the poised epigenetic states contribute to configure different subtypes of breast cancer. Such epigenetic states in TNBC could acquire differentiated cysteine requirements in cells and dictate cancer cells with distinct cellular responses to cysteine deprivation. In addition, epigenetic changes during therapy are potential drivers of therapeutic drug resistance in cancer [39]. Therefore, modulation of epigenetic regulator's activity could render cysteine dependence and overcome drug resistance in tumor cells.

In this study, we found that the expression levels of claudin genes correlate with cysteine-dependence in TNBC and claudin-high TNBC cells are resistant to cysteine deprivation. We identified HDAC6 inhibitors as potent sensitizers by drug screening to overcome the drug resistance of cysteine depletion in claudin-high tumor cells. Moreover, HDAC6 inhibitors, independent on their canonical target HDAC6, promote synthetic lethality of cysteine depletion through activation of PKCγ signaling. Our study revealed a new function of HDAC6 inhibitors that could be used as therapeutic adjuvants for the targeted cysteine-dependence therapy to treat various subtypes of breast cancer.

Methods

Cell culture and reagents

All breast tumor cells and 293T cells were purchased from ATCC and maintained as per standard protocol in an incubator with 95% humidity and 5% CO_2 at 37^{o}C. Cells were cultured in DMEM with 10% heat-inactivated fetal bovine serum (FBS) and 1% penicillin-streptomycin. The cysteine deficient medium was prepared according to the previous report [40]. Erastin, selective HDAC6 inhibitors tubacin, tubastatin A, and CAY10603, Myriocin, and the metal chelator *N*, *N*, *N*′, *N*′-tetrakis (2-pyridylmethyl) ethylenediamine (TEPN) were obtained from Cayman Chemicals (Ann Arbor, Michigan, US); Z-VAD-FMK, necrostatin-1, and ferrostatin-1 were purchased from Calbiochem Research Biochemicals (Sigma). The molecular probe FluoZin-3 was purchase from Thermo Fisher Scientific. All antibodies used in this study were listed in supplementary table 1.

2.2 Epigenetic compound library screening

Breast tumor cells HCC38 or T47D were seeded in two sets of epigenetic compound library plates under either cystine-rich or cystine depleted condition respectively. The cell viability was determined at 72 hours using the CellTiter-Glo assay kit (Promega).

2.3 Lentiviral cell infection

Viral particles were generated in 293T cells by transfecting lentiviral packaging plasmids using Lipofectamine 3000 (ThermoFisher Scientific) and collected from cell media after 48 hours. The targeted

cells were infected for 48 hours by indicated viruses and further stably selected by either puromycin or blasticidin (Cayman chemical). The pLentiCRISPR-v2-HDAC6 was purchased from GenScript with the targeting sgRNA sequence 5'-CAGTGCTACAGTCTCGCAC. All shRNAs targeting HDAC6 and PRKCG genes were purchased from Sigma. The pLKO1.0 plasmid was used as a control vector for infection.

Gene expression profiling and geneset enrichment analyses (GSEA)

The gene expression profile in HCC38 cells treated with either control, erastin, tubacin, or erastin and tubacin for 24 hours was analyzed by the GeneChip™ Human Gene 2.1 ST 24-Array Plate (ThermoFisher Scientific). The data were deposited in GEO database (GSE154425). The probe intensities were normalized by RMA. The gene expression changes in HCC38 cells were derived by zero-transformation ($\Delta\log_2$) against those in the control condition. Probe sets that varied by 2-fold in at least 3 samples were selected for hierarchical clustering. The pathway enrichment was analyzed by Gene Set Enrichment Analysis (GSEA) using the G2 annotated-genesets with default criteria of 1000 permutations.

RNA extraction and real-time RT-PCR

RNA was extracted from cells by RNeasy kit (Invitrogen). Total RNA (2 μg) was reverse-transcribed to cDNA and the quantitative PCR was performed using SYBR Green PCR mix (Applied Biosystems). The relative difference in mRNA expression was normalized with actin using the ΔΔCT method. All primers in this study were listed in supplementary table 2.

Protein immunoblotting analysis

Proteins were extracted from the cells using the RIPA extraction and lysis buffer (Sigma) with the protease and phosphatase inhibitor cocktail (ThermoFisher Scientific). Protein concentrations were determined by BCA protein assay. Equal amounts of protein were loaded for the immunoblot analyses. The signal was detected by the ECL plus Western blotting detection system (Amersham) and visualized by LAS-4000 lumino image analyzer.

Cell viability and cytotoxicity

Cell viability was measured by either trypan blue cell counting or the relative ATP level using the CellTiter-Glo assay kit (Promega) and evaluated by crystal violet staining. Cell cytotoxicity was measured using the CytoTox-Fluor™ cytotoxicity assay kit (Promega).

Microscopic Imaging

To analyze intracellular zinc levels, 7×10^3 cells were seeded in the 96-well plate under various treatments. In the end, the cells were stained by 2 μM FluoZin-3 molecular probe (ThermoFisher Scientific) at 37 °C for 30 min. Dialyzed FBS medium was used to ensure that the medium was zinc-free. Then cells were stained by 1 μM of 4',6-diamidino-2-phenylindole (DAPI) for 5 min. Cells were imaged by ZOE™ Fluorescent Cell Imager microscopy.

Cellular zinc level measurement

Total cellular zinc including labile and bound zinc was determined using ICP-OES (CHORI Elemental Analysis Facility) [41]. Briefly, 3×10^6 HCC38 cells under different treatments were collected and fully dissolved in 0.25 mL OmniTrace 70% HNO_3 (EMD Chemicals) by microwave digestion. Samples were diluted to 5% HNO_3 with OmniTrace water and analyzed with the use of a Vista Pro ICP-OES (Varian Vista Pro). Zinc was measured at the 213-nm wavelength with a detection range between 0.005 and 5 ppm. All associated reagents and plasticware were certified as trace metal-free or tested for trace metal contamination. Zinc concentrations were normalized by total protein mass. All samples were analyzed in triplicate.

Statistical analyses

The significance of differences between groups was determined using a *t* test. Statistical analysis was performed using GraphPad Prism 8.0 Software. A *p*-value < 0.05 was considered statistically significant. Data were presented in figures as mean ± standard deviation (SD).

Results

HDAC6 inhibitors sensitize the claudin-high TNBCs to cysteine deprivation

Cysteine dependence/addiction is a novel feature in mostly aggressive TNBC cells [42]. However, only a subset of TNBC exhibited cysteine-dependence, such as HBL100 and MDA-MB-231 cells, which underwent rapid necrotic cell death in response to erastin, an inhibitor of cysteine transport, while HCC70 and HCC38 cells exhibited no significant cell death (**Fig. S1A**). To examine whether gene expression programs correlate differential cysteine requirement in TNBC, the gene expression profiling data of various TNBC cells (GSE69017) [43] were subjected to the cluster analysis. We found that two subgroups of TNBCs, with differentiated claudin gene expression, correlated with their cysteine-dependence, which were named claudin-high and claudin-low TNBC (**Fig. S1B**),. Gene Set Enrichment Analysis (GSEA) showed that the claudin-high TNBC has high epithelial gene expressions but low metastasis-related gene expressions, such as epithelial-mesenchymal transition (EMT) markers *CDH1* and *VIM* (**Fig. S1C and S1D**), which were confirmed by quantitative RT-PCR (**Fig. S1F**). The genes with potential DNA and histone methylation in their promoters are suppressed in claudin-low TNBC cells (**Fig. S1E**), suggesting a role of epigenetic regulation in cell identity. In addition, analysis of gene profiling data from 812 TCGA invasive breast carcinoma tumors [44] indicated that the claudin genes are highly correlated with each other but have less or no correlation with the EMT markers *CDH1* and *VIM* (**Fig. S1G**). These data suggest that the claudin genes should be supportive or better biomarkers to determine tumor cysteine-dependence *in vivo*.

Epigenetic regulation could determine cysteine-dependence in TNBC, since epigenetic alterations are often associated with cancer progression and therapeutic drug-resistance in breast tumors [36–38]. To

overcome the drug resistance in claudin-high TNBCs, we examined whether modulation of epigenetic regulator's activity can sensitize cysteine-independent tumor cells to cystine depletion. To that end, we developed a synthetic-lethal library screen strategy, by which the cell survival rate of cysteine-independent and claudin-high cancer cells was examined under cotreatment of epigenetic inhibitor and cystine deprivation. 140 inhibitors of epigenetic regulators were included in the epigenetic compound library, and the screening was performed in claudin-high TNBC (HCC38) and luminal (T47D) cancer cells. The epigenetic compound (2 μM) was applied to these cells in either cystine-replete (+ Cys) or cystine-depleted (-Cys) condition and cell survival was measured by cellular ATP levels. By drug screening, three inhibitors of the histone deacetylase 6 (HDAC6), Tubacin, CAY10603, and Tubastatin A, were identified and dramatically induced synthetic-lethal death in both HCC38 and T47D cells under the cystine-depleted condition (Fig. 1A and 1B). We confirmed that tubacin indeed induced significant synthetic cell death in claudin-high TNBC MDA-MB-436 and HCC70 cells when cotreated with either cysteine deprivation or erastin, while either tubucin or erastin alone had no significant cytotoxicity (Fig. 1C-D and S2A-B). To further consolidate our observations, we found that tubacin plus erastin also induced massive cell death in additional claudin-high tumor cells, including luminal and Her-2 positive breast tumor cells (Fig. 1E-F and S2C). Similar as tubacin, Cay10603 significantly promoted the lethal effects of erastin in claudin-high TNBCs (Fig. 1G-H and S2D). Taken together, our drug screening identified HDAC6 inhibitors as potent sensitizers to promote synthetic lethality of cysteine depletion.

HDAC6 inhibitors synergize with erastin to induce a mixed necrotic and apoptotic cell death

To characterize the synthetic-lethal death pathway induced by erastin and HDAC6 inhibitors, we examined various death and signaling markers and protective effects of different cell death inhibitors. The combined erastin and tubacin treatment caused activation of death signaling (phosphorylation of p38) and increase of DNA double-strand breaks (phosphorylation of H2AX) with a partial cleavage of PARP1 and caspase-3 (Fig. 2A and 2B), while either erastin or tubacin treatment alone failed to activate such death markers and signaling. Acetylation of α-tubulin, the substrate of HDAC6, was strongly induced by tubacin. The synergistic cell death was only partially blocked by the pan-caspase inhibitor Q-Vad, but fully rescued by the ferroptosis and necroptosis inhibitors Ferrostatin-1 and Necrostatin-1 (Fig. 2C-D), and which abolished most cell death markers and signaling (Fig. 2E), indicating a largely necrotic cell death or ferroptosis. Similarly, the cell lethal effects induced by CAY10603 was blocked by all three cell death inhibitors (Fig. 2F). These data suggested that HDAC6 inhibitors synergize with erastin induced a mixed necrotic and apoptotic cell death program in cysteine-independent tumor cells.

HDAC6 is not required for tubacin to promote synergistic cell death.

HDAC6 has been suggested as a therapeutic target since high level of HDAC6 has been reported in small-size and ER/PR positive breast tumors and to confer drug resistance [45, 46]. Therefore, we determined whether inactivation of endogenous HDAC6's activity by shRNA is able to mimic the lethality-promoting effect of HDAC6 inhibitors in our context. Unexpectedly, silencing of HDAC6 expression by different

shRNAs did not promote cell death in response to erastin, although the protein level of HDAC6 was knocked down and the acetylation level of tubulin protein was significantly increased (**Fig. S3A-C**). We questioned whether shRNA is unable to inactivate HDAC6 enough to the same level of HDAC6 inhibitors. To that end, we employed CRISPR/Cas9 gene editing to knockout HDAC6 expression in claudin-high TNBC HCC38 and MDA-MB-436 cells and luminal T47D cancer cells. Independent HDAC6-null cell clones were isolated based on the complete deletion of HDAC6 protein expression and increased acetylation of tubulin (Fig. 3A-C upper panel). Surprisingly, knockout of HDAC6 could not promote the synthetic-lethal response with erastin, which was shown by no significant ATP decrease and cell loss in different HDAC6-null cell clones (Fig. 3A-C lower panel and **3E**). Erastin with tubacin, but not erastin alone, induced similar cell death (Fig. 3A-C lower panel and **3E**) and activated similar death markers (Fig. 3D) in both HDAC6-null and vector cells. The sphingolipid biosynthesis was previously identified as a so-called off-target of tubacin [47]. However, myriocin, an inhibitor of sphingolipid synthesis, failed to promote cell death with erastin in cysteine-independent tumor cells (**Fig. S3D-E**). We excluded the involvement of sphingolipid biosynthesis in this context. Taken together, the data strongly suggest that the death-promoting effect of HDAC6 inhibitors is independent on endogenous HDAC6.

Tubacin synergizes with erastin to activate a lethal gene transcriptional program

Although the molecular target(s) of HDAC6 inhibitors in our system remains elusive, dissecting the HDAC6 inhibitors-mediated gene transcriptional program might uncover the underlying death-promoting mechanism and help to identify new molecular targets of HDAC6 inhibitors. To that end, we examined the gene expression profiling in HCC38 cells under various conditions by Affymetrix microarray (Human Gene 2.1 ST Array). RNA was collected from cells in triplicate treated with either control, erastin, tubacin, or erastin plus tubacin and subjected to microarray analysis (GSE154425). By the supervised cluster analysis, we found that either erastin or tubucin alone induced mild or few changes of gene expression. However, the combination of tubacin and erastin dramatically triggered induction or repression of a large group of genes (Fig. 4A), such as apoptotic genes *(Bim*, *BNIP3*, and *Puma*) and genes involved in endoplasmic reticulum and oxidative stress (*ATF3*, *CHOP*, and *HOMX1*). GSEA revealed that the gene response induced by tubacin and erastin mimics the gene changes by photodynamic therapy (PDT) **(**Fig. 4B**)**, which is a well-established cancer therapy utilizing a light-absorbing molecule or visible light irradiation to cause tumor ablation [48]. RT-qPCR and immunoblotting data confirmed the profiling data that the apoptotic genes were strongly induced by the combination treatment, but not by either erastin or tubacin alone (Fig. 4C-D). Similarly, erastin alone did not activate apoptotic genes in the HDAC6-null cells (Fig. 4E-F). These data suggested that tubacin and erastin induces a lethal gene response but in an HDAC6-independent manner.

HDAC6 inhibitors synergize with erastin induce cellular zinc response.

Ferroptosis is a new form of necrotic cell death, iron-dependent and characterized by the accumulation of lipid peroxidation products and reactive oxygen species (ROS) [49, 50]. We did not find any changes in

genes involved in cellular iron metabolism. Interestingly, the genes involved in zinc transport and storage, such as ZnT1, ZnT2, and the metallothioneins MT1G/1H/1M, were highly induced by erastin and tubacin (Fig. 4A). RT-qPCR confirmed that these zinc-related genes were strongly induced by the combined treatment, but not by either erastin or tubacin alone (Fig. 5A-B). Similarly, Cay10603 along with erastin also strongly activated the zinc-related genes (Fig. 5C). Previous reports showed that the increase of zinc in cells causes ROS production and induces a mixed type of cell death, including apoptosis and necrosis [51, 52]. Therefore, we examined whether the zinc is involved in tubacin mediated death-promoting effects. The FluoZin™-3, a Zn^{2+}-selective indicator, was used to detect cellular labile zinc. Indeed, the level of labile zinc was highly increased in cells by erastin and tubacin, but not significantly by either erastin or tubacin alone (Fig. 5D and S4A). Increased labile zinc mostly accumulated in nucleus, as it co-localized with nuclear DNA stained by DAPI. Next, the total cellular level of zinc, including labile and bound zinc, was determined by ICP-OES. We found that the total cellular level of zinc was not significantly altered under any conditions (Fig. 5E). These suggested that the increased labile zinc was mostly released from cellular proteins or compartments but not imported from culture media. To test whether the increased labile zinc mediated the death-promoting effects, TPEN, a zinc ion chelator [53], was used to chelate the labile zinc in cells. However, TPEN could not protect cells from cell death induced by erastin with tubacin (Fig. 5F and S4B). In summary, these results suggested that the zinc-related gene response and increase of labile zinc are likely the outcomes of cell death, but not the death-promoting mechanism of HDAC6 inhibitors.

Inhibition of PKC suppresses the death-promoting effects of tubucin in claudin-high TNBC

Since zinc can function as a structural or modulatory component of many regulatory and signaling proteins [54, 55], the increase of labile zinc in cells could indicate alterations of cellular protein function or signaling. Previous reports indicated that the zinc release from protein kinase C (PKC) is a common event during PKC activation by reactive oxygen species [56, 57]. Therefore, we examined whether activation of PKC is required for the death-promoting effects of HDAC6 inhibitors. We found that Gö 6983, a PKC inhibitor with a broad inhibitory spectrum [58], fully rescued cells from cell death induced by erastin and tubacin, while Gö 6976, a selective inhibitor of PKCα/β, had no protective role (Fig. 6A and S5A). Immunoblotting and RT-qPCR analysis confirmed that Gö 6983 abolished the induction of cell death genes and phosphorylation of PKC substrates triggered by the combined erastin and tubacin (Fig. 6B-C and S5B). Moreover, Gö 6983 significantly suppressed the zinc-related gene response and increase of labile zinc in cells (Fig. 6D-E and S5C). These results suggested that activation of PKC, but not PKCα/β, is required for tubacin to promote cell death in cysteine-independent cells.

PKCγ is required for the tubacin-mediated synthetic-lethality

Next, we examined which member of PKC family kinases is required for the death-promoting effects of tubacin. Two additional PKC inhibitors with a slightly different inhibitory spectrum, bisindolylmaleimide I

and sotrastaurin, were used. Similar to Gö 6983, bisindolylmaleimide I strongly protected cells from cell death induced by erastin and tubacin, but sotrastaurin failed to rescue cells from the stress (Fig. 7A-B). Based on the protective role and inhibitory spectrum of various PKC inhibitors, PKCγ is the candidate kinase since it is inhibited by Gö 6983 and bisindolylmaleimide I, but not by Gö 6976 and sotrastaurin. Immunoblotting analysis showed that there was a transient phosphorylation of PKCγ in the early phase during the combined erastin and tubacin treatment, which was associated with the phosphorylation of PKC substrates, while the phosphorylation of PKC δ/θ occurred in the later phase (Fig. 7C). Furthermore, knockdown of PKCγ by shPKCγ significantly alleviated cell death induced by erastin and tubacin in cysteine-independent TNBCs (Fig. 7D and 7F). In consistent with its protective role, PKCγ knockdown suppressed induction of cell death genes and phosphorylation of H2AX (Fig. 7E). Taken together, activation of PKCγ is required for the tubacin-promoting synthetic-lethality in cysteine-independent TNBCs.

Discussion

TNBC is the most challenging subtype of breast cancer and overall its survival rate remains very low [59]. Developing novel targeted therapies and defining associated biomarkers are urgent needed for precise TNBC treatment. Targeting cysteine-dependence can eradicate a subset of TNBCs with highly epithelial-to-mesenchymal transition (EMT) but less responsive in many other TNBCs and luminal breast cancer [42]. The early reports indicated that the claudin-low tumors are an aggressive subtype of breast cancer with poor prognosis that enriches tumor-initiating cells with high expression of EMT markers [60, 61]. Our gene expression analysis showed that the expression of claudin genes, such as *CLDN 3*, *CLDN4*, and *CLDN7*, are highly correlated with classical EMT markers *CDH1* and *VIM* genes *in vitro* and can differentiate cysteine-dependence in TNBC. However, the expression of claudins are highly correlated with each other in invasive breast tumors *in vivo*, but not greatly correlated with the expression of *CDH1* and *VIM.* This discrepancy suggests that the claudin genes should be used as additional biomarkers to guide the precise application of targeted cysteine-dependence therapy in TNBC patients.

Since many TNBC and luminal breast cancer are cysteine-independent, optimization of targeted cysteine-dependence therapy will be required for its broad and effective application. Epigenetic alterations can change tumor identity and metabolism, contribute to breast tumor heterogeneity, and acquire drug resistance in cancer [36, 38]. Many epigenetic activators or inhibitors have been used as therapeutic adjuvants to increase chemotherapy efficacy and overcome drug resistance [34, 39]. In line with these, we identified that the HDAC6 inhibitors can render cysteine-independent tumor cells sensitive to cysteine deprivation. HDAC6 is a unique member of the HDAC family that can regulate cell proliferation, metastasis, and invasion in tumors, and can also drive tumor progression and confer drug resistance in some cancers [62–65]. These observations suggest that HDAC6 is likely a reasonable molecular target in our system. However, we showed that knockout of endogenous HDAC6 protein did not mimic HDAC6 inhibitors to synergize with erastin to induce cell death in claudin-high TNBC. This indicates that the synergistic effect of HDAC6 inhibitors is via a new cellular molecule, which is entirely independent of HDAC6. Previous report showed that the sphingosine biosynthesis is an off-target of tubacin [66], but we

ruled out the involvement of the sphingosine pathway in our system. More studies are needed in order to identify new molecular target(s) of HDAC6 inhibitors since identification of such new targets of HDAC6 inhibitors would help us reveal new genes or pathways involved in tumor cysteine-addiction, and which can be used as direct targets in combination with cysteine deprivation for cancer treatment. Many studies had attempted to use HDAC6 inhibitors to treat cancer, but the therapeutic outcomes of these inhibitors should be carefully examined in order to avoid any off-targeting in patients.

The intrinsic target of HDAC6 inhibitors in our context remains unknown, but we found that tubacin with erastin triggered many stress and apoptotic gene responses, one of which mimics the photodynamic therapy (PDT) gene response [48]. The tubacin-promoting cell death occurred as a mixed type of cell death, which includes apoptosis, necroptosis, and ferroptosis. Ferroptosis is an iron-dependent cell death driven by lipid peroxidation with necrotic features [28, 49, 50]. The transcriptional profiling data did not show any iron-related gene response, but a prominent zinc-related gene response was activated by the combined erastin and tubacin, which was confirmed by a significant increase of labile zinc in cells. We found total zinc, including labile and bound forms, was not significantly changed in treated cells, which indicated that increase of labile zinc was likely released from cellular proteins or compartments but not imported from extracellular culture media.

Zinc is a trace but essential metal micronutrient and is integral to many enzymes and regulatory proteins, and functions as a signaling messenger in cells [67, 68]. We found that cellular zinc homeostasis is deregulated by HDAC6 inhibitors and cysteine depletion, but the increase of labile zinc does not promote cell death. Therefore, the increase of labile zinc in cells is a possible indicator of intracellular signaling perturbations under the combined treatment. It has been reported that reactive oxygen species (ROS) can cause zinc releasing from oxidized metallothioneins and zinc-fingers of abnormal proteins [69]. More specifically, it has been shown that zinc can modulate the activity of PKC family isozymes via zinc finger domains and activation of PKCα/β by ROS stress can release zinc directly from PKC into cytoplasm [56, 57]. Different isozymes of PKC family play roles in multiple cellular processes including proliferation, survival, invasion, angiogenesis [70]. Indeed in our study, inhibition of PKC abolished the release of labile zinc and cell death. Specifically, activation of PKCγ is required for the tubacin's death-promoting effects. As one of conventional PKC isozymes, PKCγ is mainly present in the brain and has very few studies in cancer [71]. Recent studies showed that activation of PKCγ increases the migratory capacity in colon cancer [72, 73]. Our study identified a new role of PKCγ in breast cancer that the signaling of PKCγ is important to mediate the cysteine-dependence.

Conclusion

We found that cysteine-dependence in TNBC associates with the expression levels of claudin genes in addition to the classical EMT markers. HDAC6 inhibitors identified by the epigenetics compound library screening overcome drug resistance in claudin-high TNBC and promote the synthetic-lethality of cysteine deprivation. Importantly, HDAC6 inhibitors execute their death-promoting effects independent on their canonical target HDAC6 protein. In addition, HDAC6 inhibitors synergize with cysteine restriction to trigger

a mixed type of cell death by induces a profound gene transcriptional program via the PKCγ signaling. Identified such HDAC6 inhibitors will support the broad translational application of targeted cysteine-dependence therapy in various types of breast cancer.

Abbreviations

HDAC6
Histone deacetylase 6
TNBC
Triple-negative breast cancer
PKC
Protein kinase C
GSH
Glutathione
GPXs
Glutathione peroxidases
xC-
Cystine/glutamate antiporter
+Cys
Cystine-replete condition
-Cys
Cystine-depleted condition
EMT
Epithelial-mesenchymal transition
GSEA
Geneset enrichment analyses
CDH1
Cadherin 1
VIM
Vimentin
LOXL2
Lysyl Oxidase Like 2
Zeb2
Zinc Finger E-Box Binding Homeobox 2
TPEN
N, N, N′, N′-tetrakis (2-pyridylmethyl) ethylenediamine
ROS
Reactive oxygen species
ER/PR
Estrogen receptors/ progesterone receptor

MT1G/1H/1M
Metallothioneins
ZnT1
Zinc transporter 1
ZnT2
Zinc transporter 2
PDT
Photodynamic therapy
ICP-OES
CHORI Elemental Analysis Facility
ATF3
Activating Transcription Factor 3
CHOP
C/EBP homologous protein
HOMX1
Heme Oxygenase 1
Puma
p53 upregulated modulator of apoptosis
Bim
BCL2 Like 11
BNIP3
BCL2 Interacting Protein 3

Declarations

Ethics declarations

Not applicable

Consent for publication

Not applicable

Competing interests

The authors declare that they have no known competing financial interests or personal relationships that could influence the work reported in this paper.

Funding

This study was partially supported by the National Institute of Health (Grant # 1R15CA246336-01) to X.T. and the Research excellence fund of Michigan Technological University (Grant # 2015-025) to X.T.

Availability of data and materials

The datasets generated and used in the current study are available in the Gene Expression Omnibus (GEO) database (https://www.ncbi.nlm.nih.gov/geo/) and The Cancer Genome Atlas (TCGA) database (https://www.cancer.gov/about-nci/organization/ccg/research/structural-genomics/tcga).

Authors' contributions

TA and XT conceived and designed the experiments. TA and MC performed the experiments. TA and MC contributed to the acquisition of data, analysis and interpretation of data. TA and XT wrote, reviewed, and revised the manuscript. All authors read and approved the final manuscript.

Acknowledgments

We thank scientists from UNC Genomics Core Facilities for the technical support in the gene transcriptional profiling analysis.

References

1. Cancer Genome Atlas N: **Comprehensive molecular portraits of human breast tumours**. *Nature* 2012, **490**(7418):61-70.
2. Bieche I, Lidereau R: **Genome-based and transcriptome-based molecular classification of breast cancer**. *Curr Opin Oncol* 2011, **23**(1):93-99.
3. Dai X, Li T, Bai Z, Yang Y, Liu X, Zhan J, Shi B: **Breast cancer intrinsic subtype classification, clinical use and future trends**. *Am J Cancer Res* 2015, **5**(10):2929-2943.
4. Weigelt B, Peterse JL, van 't Veer LJ: **Breast cancer metastasis: markers and models**. *Nat Rev Cancer* 2005, **5**(8):591-602.
5. DeSantis C, Siegel R, Bandi P, Jemal A: **Breast cancer statistics, 2011**. *CA Cancer J Clin* 2011, **61**(6):409-418.
6. Bray F, Ferlay J, Soerjomataram I, Siegel RL, Torre LA, Jemal A: **Global cancer statistics 2018: GLOBOCAN estimates of incidence and mortality worldwide for 36 cancers in 185 countries**. *CA Cancer J Clin* 2018, **68**(6):394-424.
7. Mayer IA, Abramson VG, Lehmann BD, Pietenpol JA: **New strategies for triple-negative breast cancer—deciphering the heterogeneity**. *Clinical cancer research* 2014, **20**(4):782-790.
8. Neophytou C, Boutsikos P, Papageorgis P: **Molecular Mechanisms and Emerging Therapeutic Targets of Triple-Negative Breast Cancer Metastasis**. *Front Oncol* 2018, **8**:31.
9. Ogrodzinski MP, Bernard JJ, Lunt SY: **Deciphering metabolic rewiring in breast cancer subtypes**. *Transl Res* 2017, **189**:105-122.
10. Xu H, Eirew P, Mullaly SC, Aparicio S: **The omics of triple-negative breast cancers**. *Clin Chem* 2014, **60**(1):122-133.

11. Wahba HA, El-Hadaad HA: **Current approaches in treatment of triple-negative breast cancer**. *Cancer Biol Med* 2015, **12**(2):106-116.
12. Banerji S, Cibulskis K, Rangel-Escareno C, Brown KK, Carter SL, Frederick AM, Lawrence MS, Sivachenko AY, Sougnez C, Zou L *et al*: **Sequence analysis of mutations and translocations across breast cancer subtypes**. *Nature* 2012, **486**(7403):405-409.
13. Shah SP, Roth A, Goya R, Oloumi A, Ha G, Zhao Y, Turashvili G, Ding J, Tse K, Haffari G *et al*: **The clonal and mutational evolution spectrum of primary triple-negative breast cancers**. *Nature* 2012, **486**(7403):395-399.
14. Hanahan D, Weinberg RA: **Hallmarks of cancer: the next generation**. *Cell* 2011, **144**(5):646-674.
15. Hainaut P, Plymoth A: **Targeting the hallmarks of cancer: towards a rational approach to next-generation cancer therapy**. *Curr Opin Oncol* 2013, **25**(1):50-51.
16. Lunt SY, Vander Heiden MG: **Aerobic glycolysis: meeting the metabolic requirements of cell proliferation**. *Annual review of cell and developmental biology* 2011, **27**:441-464.
17. Sreekumar A, Poisson LM, Rajendiran TM, Khan AP, Cao Q, Yu J, Laxman B, Mehra R, Lonigro RJ, Li Y *et al*: **Metabolomic profiles delineate potential role for sarcosine in prostate cancer progression**. *Nature* 2009, **457**(7231):910-914.
18. Tang X, Lin CC, Spasojevic I, Iversen ES, Chi JT, Marks JR: **A joint analysis of metabolomics and genetics of breast cancer**. *Breast Cancer Res* 2014, **16**(4):415.
19. Song CW, Clement JJ, Levitt SH: **Preferential cytotoxicity of 5-thio-D-glucose against hypoxic tumor cells**. *J Natl Cancer Inst* 1976, **57**(3):603-605.
20. Akins NS, Nielson TC, Le HV: **Inhibition of Glycolysis and Glutaminolysis: An Emerging Drug Discovery Approach to Combat Cancer**. *Curr Top Med Chem* 2018, **18**(6):494-504.
21. Yuneva M, Zamboni N, Oefner P, Sachidanandam R, Lazebnik Y: **Deficiency in glutamine but not glucose induces MYC-dependent apoptosis in human cells**. *J Cell Biol* 2007, **178**(1):93-105.
22. Wise DR, DeBerardinis RJ, Mancuso A, Sayed N, Zhang XY, Pfeiffer HK, Nissim I, Daikhin E, Yudkoff M, McMahon SB *et al*: **Myc regulates a transcriptional program that stimulates mitochondrial glutaminolysis and leads to glutamine addiction**. *Proc Natl Acad Sci U S A* 2008, **105**(48):18782-18787.
23. Dixon SJ, Lemberg KM, Lamprecht MR, Skouta R, Zaitsev EM, Gleason CE, Patel DN, Bauer AJ, Cantley AM, Yang WS *et al*: **Ferroptosis: an iron-dependent form of nonapoptotic cell death**. *Cell* 2012, **149**(5):1060-1072.
24. Tang X, Wu J, Ding CK, Lu M, Keenan MM, Lin CC, Lin CA, Wang CC, George D, Hsu DS *et al*: **Cystine Deprivation Triggers Programmed Necrosis in VHL-Deficient Renal Cell Carcinomas**. *Cancer Res* 2016, **76**(7):1892-1903.
25. Badgley MA, Kremer DM, Maurer HC, DelGiorno KE, Lee HJ, Purohit V, Sagalovskiy IR, Ma A, Kapilian J, Firl CEM *et al*: **Cysteine depletion induces pancreatic tumor ferroptosis in mice**. *Science* 2020, **368**(6486):85-89.

26. Bansal A, Simon MC: **Glutathione metabolism in cancer progression and treatment resistance**. *J Cell Biol* 2018, **217**(7):2291-2298.
27. Li J, Cao F, Yin HL, Huang ZJ, Lin ZT, Mao N, Sun B, Wang G: **Ferroptosis: past, present and future**. *Cell Death Dis* 2020, **11**(2):88.
28. Stockwell BR, Friedmann Angeli JP, Bayir H, Bush AI, Conrad M, Dixon SJ, Fulda S, Gascon S, Hatzios SK, Kagan VE *et al*: **Ferroptosis: A Regulated Cell Death Nexus Linking Metabolism, Redox Biology, and Disease**. *Cell* 2017, **171**(2):273-285.
29. Lo M, Ling V, Low C, Wang YZ, Gout PW: **Potential use of the anti-inflammatory drug, sulfasalazine, for targeted therapy of pancreatic cancer**. *Curr Oncol* 2010, **17**(3):9-16.
30. Doxsee DW, Gout PW, Kurita T, Lo M, Buckley AR, Wang Y, Xue H, Karp CM, Cutz JC, Cunha GR *et al*: **Sulfasalazine-induced cystine starvation: potential use for prostate cancer therapy**. *Prostate* 2007, **67**(2):162-171.
31. Graczyk-Jarzynka A, Zagozdzon R, Muchowicz A, Siernicka M, Juszczynski P, Firczuk M: **New insights into redox homeostasis as a therapeutic target in B-cell malignancies**. *Curr Opin Hematol* 2017, **24**(4):393-401.
32. Cramer SL, Saha A, Liu J, Tadi S, Tiziani S, Yan W, Triplett K, Lamb C, Alters SE, Rowlinson S *et al*: **Systemic depletion of L-cyst(e)ine with cyst(e)inase increases reactive oxygen species and suppresses tumor growth**. *Nat Med* 2017, **23**(1):120-127.
33. Tang X, Ding CK, Wu J, Sjol J, Wardell S, Spasojevic I, George D, McDonnell DP, Hsu DS, Chang JT *et al*: **Cystine addiction of triple-negative breast cancer associated with EMT augmented death signaling**. *Oncogene* 2017, **36**(30):4235-4242.
34. Dworkin AM, Huang TH, Toland AE: **Epigenetic alterations in the breast: Implications for breast cancer detection, prognosis and treatment**. *Semin Cancer Biol* 2009, **19**(3):165-171.
35. Rodenhiser DI, Andrews J, Kennette W, Sadikovic B, Mendlowitz A, Tuck AB, Chambers AF: **Epigenetic mapping and functional analysis in a breast cancer metastasis model using whole-genome promoter tiling microarrays**. *Breast Cancer Res* 2008, **10**(4):R62.
36. Feinberg AP: **Phenotypic plasticity and the epigenetics of human disease**. *Nature* 2007, **447**(7143):433-440.
37. Elsheikh SE, Green AR, Rakha EA, Powe DG, Ahmed RA, Collins HM, Soria D, Garibaldi JM, Paish CE, Ammar AA *et al*: **Global histone modifications in breast cancer correlate with tumor phenotypes, prognostic factors, and patient outcome**. *Cancer Res* 2009, **69**(9):3802-3809.
38. Maruyama R, Choudhury S, Kowalczyk A, Bessarabova M, Beresford-Smith B, Conway T, Kaspi A, Wu Z, Nikolskaya T, Merino VF *et al*: **Epigenetic regulation of cell type-specific expression patterns in the human mammary epithelium**. *PLoS Genet* 2011, **7**(4):e1001369.
39. Brown R, Curry E, Magnani L, Wilhelm-Benartzi CS, Borley J: **Poised epigenetic states and acquired drug resistance in cancer**. *Nat Rev Cancer* 2014, **14**(11):747-753.
40. Tang X, Keenan MM, Wu J, Lin CA, Dubois L, Thompson JW, Freedland SJ, Murphy SK, Chi JT: **Comprehensive profiling of amino acid response uncovers unique methionine-deprived response**

dependent on intact creatine biosynthesis. *PLoS Genet* 2015, **11**(4):e1005158.

41. Killilea DW, Rohner F, Ghosh S, Otoo GE, Smith L, Siekmann JH, King JC: **Identification of a Hemolysis Threshold That Increases Plasma and Serum Zinc Concentration**. *J Nutr* 2017, **147**(6):1218-1225.
42. Tang X, Ding C-K, Wu J, Sjol J, Wardell S, Spasojevic I, George D, McDonnell D, Hsu D, Chang JJO: **Cystine addiction of triple-negative breast cancer associated with EMT augmented death signaling**. 2017, **36**(30):4235.
43. Neve RM, Chin K, Fridlyand J, Yeh J, Baehner FL, Fevr T, Clark L, Bayani N, Coppe JP, Tong F *et al*: **A collection of breast cancer cell lines for the study of functionally distinct cancer subtypes**. *Cancer Cell* 2006, **10**(6):515-527.
44. Ciriello G, Gatza ML, Beck AH, Wilkerson MD, Rhie SK, Pastore A, Zhang H, McLellan M, Yau C, Kandoth C *et al*: **Comprehensive Molecular Portraits of Invasive Lobular Breast Cancer**. *Cell* 2015, **163**(2):506-519.
45. Zhang Z, Yamashita H, Toyama T, Sugiura H, Omoto Y, Ando Y, Mita K, Hamaguchi M, Hayashi S, Iwase H: **HDAC6 expression is correlated with better survival in breast cancer**. *Clin Cancer Res* 2004, **10**(20):6962-6968.
46. Wang Z, Tang F, Hu P, Wang Y, Gong J, Sun S, Xie C: **HDAC6 promotes cell proliferation and confers resistance to gefitinib in lung adenocarcinoma**. *Oncol Rep* 2016, **36**(1):589-597.
47. Siow D, Wattenberg B: **The histone deacetylase-6 inhibitor tubacin directly inhibits de novo sphingolipid biosynthesis as an off-target effect**. *Biochem Biophys Res Commun* 2014, **449**(3):268-271.
48. Buytaert E, Matroule JY, Durinck S, Close P, Kocanova S, Vandenheede JR, de Witte PA, Piette J, Agostinis P: **Molecular effectors and modulators of hypericin-mediated cell death in bladder cancer cells**. *Oncogene* 2008, **27**(13):1916-1929.
49. Xie Y, Hou W, Song X, Yu Y, Huang J, Sun X, Kang R, Tang D: **Ferroptosis: process and function**. *Cell Death Differ* 2016, **23**(3):369-379.
50. Yang WS, Stockwell BR: **Ferroptosis: Death by Lipid Peroxidation**. *Trends Cell Biol* 2016, **26**(3):165-176.
51. Bishop GM, Dringen R, Robinson SR: **Zinc stimulates the production of toxic reactive oxygen species (ROS) and inhibits glutathione reductase in astrocytes**. *Free Radic Biol Med* 2007, **42**(8):1222-1230.
52. Hamatake M, Iguchi K, Hirano K, Ishida R: **Zinc induces mixed types of cell death, necrosis, and apoptosis, in molt-4 cells**. *J Biochem* 2000, **128**(6):933-939.
53. Cho YE, Lomeda RA, Ryu SH, Lee JH, Beattie JH, Kwun IS: **Cellular Zn depletion by metal ion chelators (TPEN, DTPA and chelex resin) and its application to osteoblastic MC3T3-E1 cells**. *Nutr Res Pract* 2007, **1**(1):29-35.
54. Maret W: **Zinc in Cellular Regulation: The Nature and Significance of "Zinc Signals"**. *Int J Mol Sci* 2017, **18**(11).

55. Slepchenko KG, Holub JM, Li YV: **Intracellular zinc increase affects phosphorylation state and subcellular localization of protein kinase C delta (delta)**. *Cell Signal* 2018, **44**:148-157.
56. Korichneva I, Hoyos B, Chua R, Levi E, Hammerling U: **Zinc release from protein kinase C as the common event during activation by lipid second messenger or reactive oxygen**. *Journal of biological chemistry* 2002, **277**(46):44327-44331.
57. Knapp LT, Klann E: **Superoxide-induced stimulation of protein kinase C via thiol modification and modulation of zinc content**. *J Biol Chem* 2000, **275**(31):24136-24145.
58. Young LH, Balin BJ, Weis MT: **Go 6983: a fast acting protein kinase C inhibitor that attenuates myocardial ischemia/reperfusion injury**. *Cardiovasc Drug Rev* 2005, **23**(3):255-272.
59. Garrido-Castro AC, Lin NU, Polyak K: **Insights into Molecular Classifications of Triple-Negative Breast Cancer: Improving Patient Selection for Treatment**. *Cancer Discov* 2019, **9**(2):176-198.
60. Fougner C, Bergholtz H, Norum JH, Sorlie T: **Re-definition of claudin-low as a breast cancer phenotype**. *Nat Commun* 2020, **11**(1):1787.
61. Hu Z, Fan C, Oh DS, Marron JS, He X, Qaqish BF, Livasy C, Carey LA, Reynolds E, Dressler L *et al*: **The molecular portraits of breast tumors are conserved across microarray platforms**. *BMC Genomics* 2006, **7**:96.
62. Li Y, Shin D, Kwon SHJTFj: **Histone deacetylase 6 plays a role as a distinct regulator of diverse cellular processes**. 2013, **280**(3):775-793.
63. Aldana-Masangkay GI, Sakamoto KM: **The role of HDAC6 in cancer**. *J Biomed Biotechnol* 2011, **2011**:875824.
64. Banik D, Noonepalle S, Hadley M, Palmer E, Gracia-Hernandez M, Zevallos-Delgado C, Manhas N, Simonyan H, Young CN, Popratiloff A *et al*: **HDAC6 Plays a Noncanonical Role in the Regulation of Antitumor Immune Responses, Dissemination, and Invasiveness of Breast Cancer**. *Cancer Res* 2020, **80**(17):3649-3662.
65. Bitler BG, Wu S, Park PH, Hai Y, Aird KM, Wang Y, Zhai Y, Kossenkov AV, Vara-Ailor A, Rauscher FJ, III *et al*: **ARID1A-mutated ovarian cancers depend on HDAC6 activity**. *Nat Cell Biol* 2017, **19**(8):962-973.
66. Chao OS, Chang TC, Di Bella MA, Alessandro R, Anzanello F, Rappa G, Goodman OB, Lorico A: **The HDAC6 Inhibitor Tubacin Induces Release of CD133(+) Extracellular Vesicles From Cancer Cells**. *J Cell Biochem* 2017, **118**(12):4414-4424.
67. Fukada T, Yamasaki S, Nishida K, Murakami M, Hirano T: **Zinc homeostasis and signaling in health and diseases: Zinc signaling**. *J Biol Inorg Chem* 2011, **16**(7):1123-1134.
68. Szewczyk B: **Zinc homeostasis and neurodegenerative disorders**. *Front Aging Neurosci* 2013, **5**:33.
69. Ruttkay-Nedecky B, Nejdl L, Gumulec J, Zitka O, Masarik M, Eckschlager T, Stiborova M, Adam V, Kizek R: **The role of metallothionein in oxidative stress**. *Int J Mol Sci* 2013, **14**(3):6044-6066.
70. Wu-Zhang AX, Newton AC: **Protein kinase C pharmacology: refining the toolbox**. *Biochem J* 2013, **452**(2):195-209.

71. Saito N, Shirai Y: **Protein kinase C gamma (PKC gamma): function of neuron specific isotype**. *J Biochem* 2002, **132**(5):683-687.

72. Dowling CM, Hayes SL, Phelan JJ, Cathcart MC, Finn SP, Mehigan B, McCormick P, Coffey JC, O'Sullivan J, Kiely PA: **Expression of protein kinase C gamma promotes cell migration in colon cancer**. *Oncotarget* 2017, **8**(42):72096-72107.

73. Parsons M, Adams JC: **Rac regulates the interaction of fascin with protein kinase C in cell migration**. *J Cell Sci* 2008, **121**(Pt 17):2805-2813.

Figures

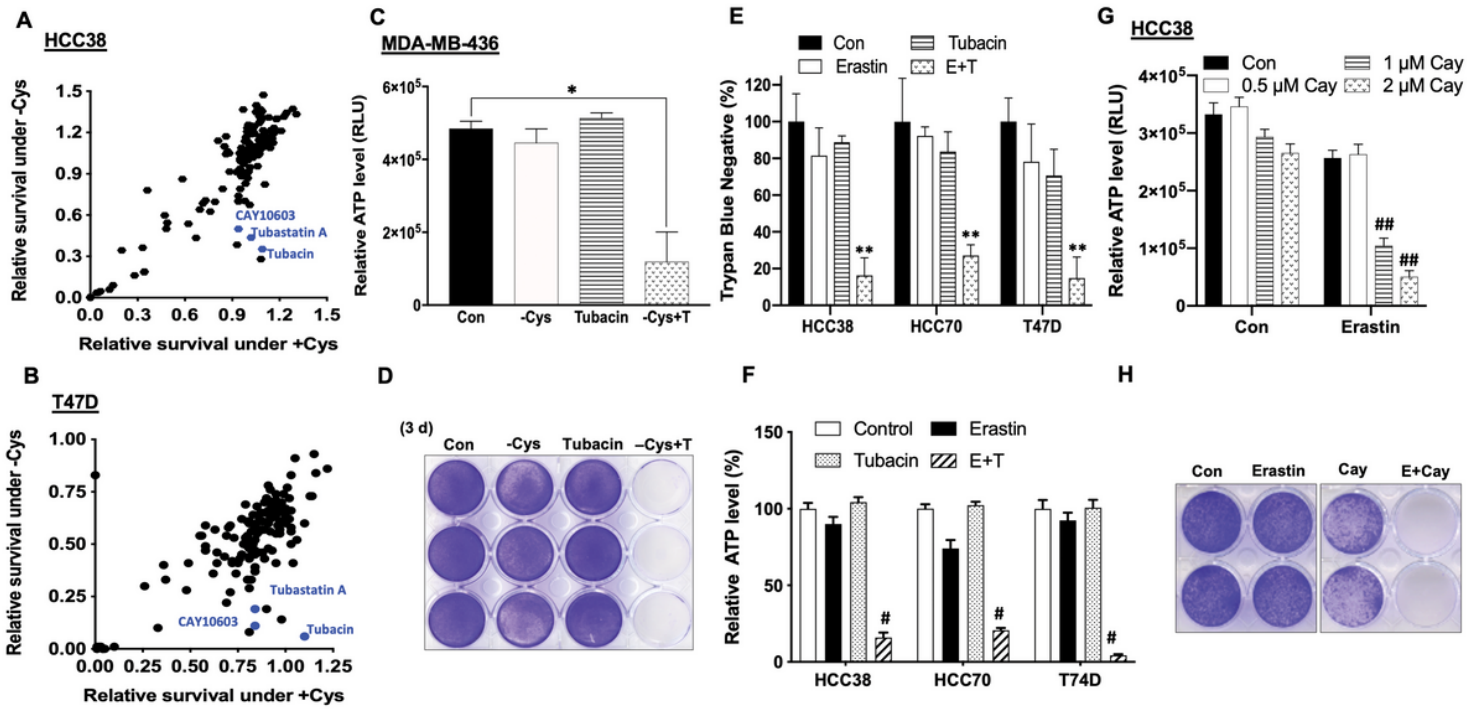

Figure 1

Epigenetic compound library screening identifies HDAC6 inhibitors to promote cell death of cystine deprivation (A, B) Relative cell survival of claudin-high TNBC HCC38 and luminal breast cancer T47D cells under cystine-depleted (-Cys) and cystine-replete (+Cys) conditions respectively with the presence of epigenetic compounds for 72 hours, which were determined by CellTiter-Glo assay. (C, D) Cell viability of claudin-high TNBC (MDA-MB-436) after exposure to cystine-replete (Con), cystine-depleted (-Cys), 5 μM tubacin (T), and 5 μM tubacin with cystine-depleted (-Cys+T) for 72 hours was measured by ATP level (C; n=3, *, $p<0.01$) or stained by crystal violet (D). (E, F) Survival rate of HCC38, HCC70, and T47D cells in response to either the control (Con), 5 μM erastin, 5 μM tubacin, or combination of erastin and tubacin (E+T) were determined by Trypan blue counting (E; **, $p<0.001$) or CellTiter-Glo assay (F; n=3, #, $p<0.001$). (G) Cell viability of HCC38 was measured by CellTiter-Glo assay after treated with the control (Con), 5 μM erastin, various concentrations of Cay10603 (Cay) 0.5, 1, and 2 μM, or combination of erastin and indicated concentration of Cay for 48h hours (n=3, ##, $p<0.005$). (H) Relative cell survival of HCC38

assessed by crystal violet staining after treated with Con, 5 μM erastin, 2 μM Cay, or combination of erastin and Cay (E+Cay) for 48 hours.

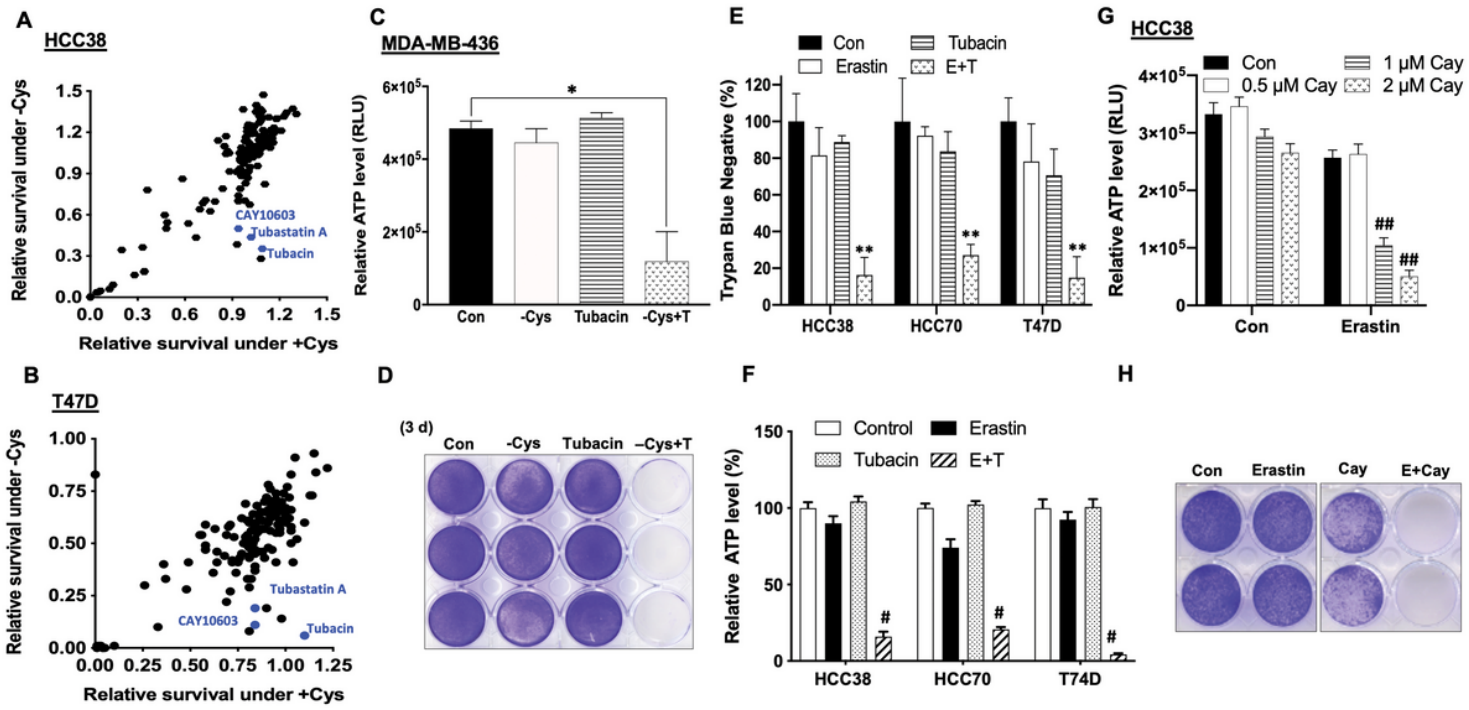

Figure 1

Epigenetic compound library screening identifies HDAC6 inhibitors to promote cell death of cystine deprivation (A, B) Relative cell survival of claudin-high TNBC HCC38 and luminal breast cancer T47D cells under cystine-depleted (-Cys) and cystine-replete (+Cys) conditions respectively with the presence of epigenetic compounds for 72 hours, which were determined by CellTiter-Glo assay. (C, D) Cell viability of claudin-high TNBC (MDA-MB-436) after exposure to cystine-replete (Con), cystine-depleted (-Cys), 5 μM tubacin (T), and 5 μM tubacin with cystine-depleted (-Cys+T) for 72 hours was measured by ATP level (C; n=3, *, $p<0.01$) or stained by crystal violet (D). (E, F) Survival rate of HCC38, HCC70, and T47D cells in response to either the control (Con), 5 μM erastin, 5 μM tubacin, or combination of erastin and tubacin (E+T) were determined by Trypan blue counting (E; **, $p<0.001$) or CellTiter-Glo assay (F; n=3, #, $p<0.001$). (G) Cell viability of HCC38 was measured by CellTiter-Glo assay after treated with the control (Con), 5 μM erastin, various concentrations of Cay10603 (Cay) 0.5, 1, and 2 μM, or combination of erastin and indicated concentration of Cay for 48h hours (n=3, ##, $p<0.005$). (H) Relative cell survival of HCC38 assessed by crystal violet staining after treated with Con, 5 μM erastin, 2 μM Cay, or combination of erastin and Cay (E+Cay) for 48 hours.

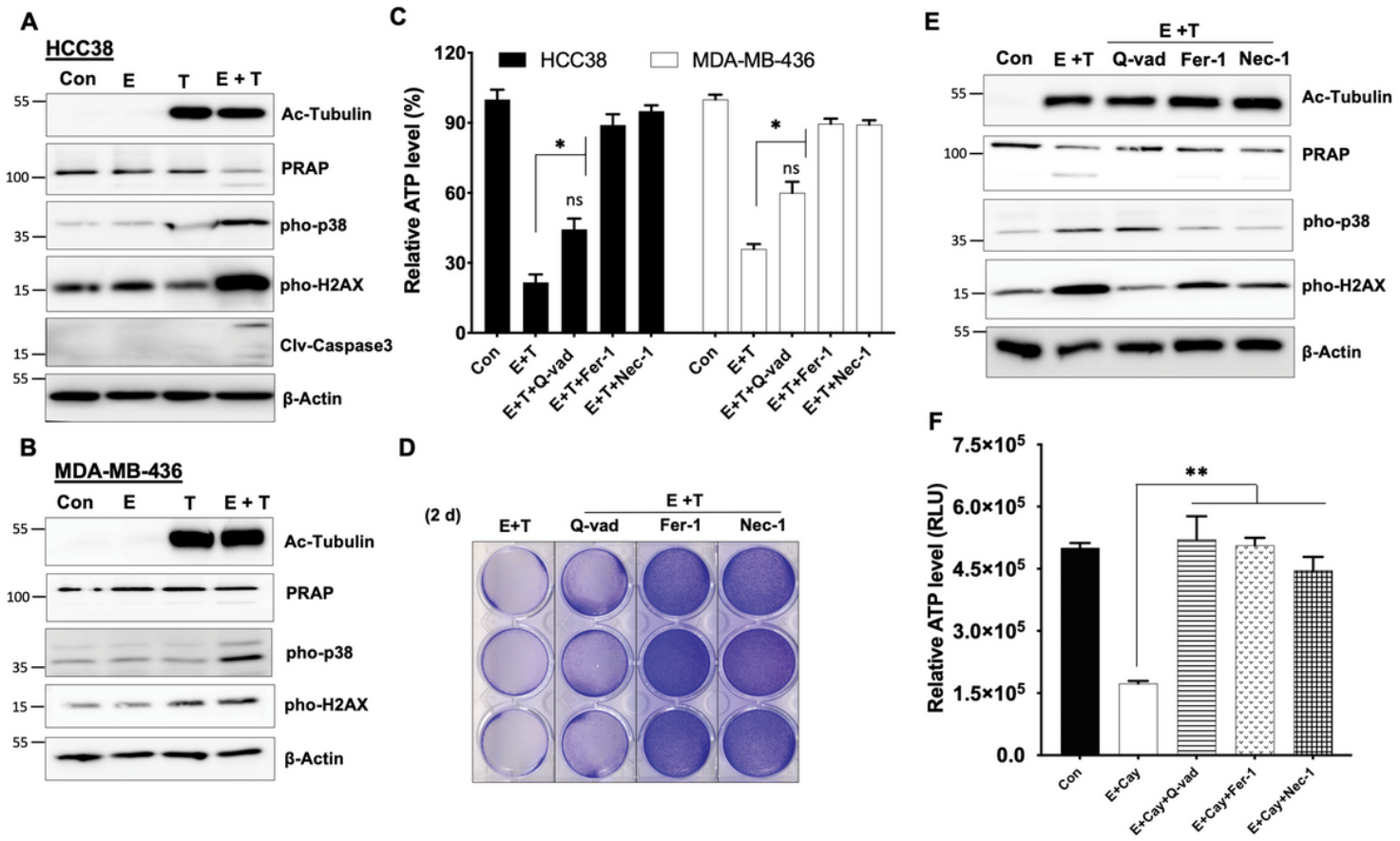

Figure 2

HDAC6 inhibitors synergize with erastin to induce a mixed type of cell death (A, B) Immunoblot analysis of acetylated-tubulin, PARP1, cleaved Caspase-3, phosphorylated p38 and H2AX protein expression in HCC38 (A; 24 hrs) and in MDA-MB-436 (B; 36 hrs) under treatments with either control (Con), 5 μM erastin (E), 5 μM tubacin (T), or combination of erastin and tubacin (E+T); -Actin serves as a protein normalization control. (C, D) Relative cell survival of HCC38 (48hrs) and MDA-MB-436 (72hrs) were measured by CellTiter-Glo assay (C; n=3, *, $p<0.001$) or HCC38 assessed by crystal violet (D) under either Con, combination of E+T, or E+T with different cell death inhibitors Q-Vad (10 μM), Fer-1(10 μM), Nec-1 (20 μM) for 48 hours. (E) Immunoblot analysis of indicated protein expression in HCC38 cells treated as (C) for 24 hours. (F) Relative cell survival was measured by CellTiter-Glo assay in HCC38 cells treated with either control (Con), combination of erastin and 2 μM Cay (E+Cay), or E+Cay with following death inhibitors Q-Vad 10 μM, Fer-1 (10 μM; **, $p<0.005$), Nec-1 (20 μM; **, $p<0.005$) for 48 hours.

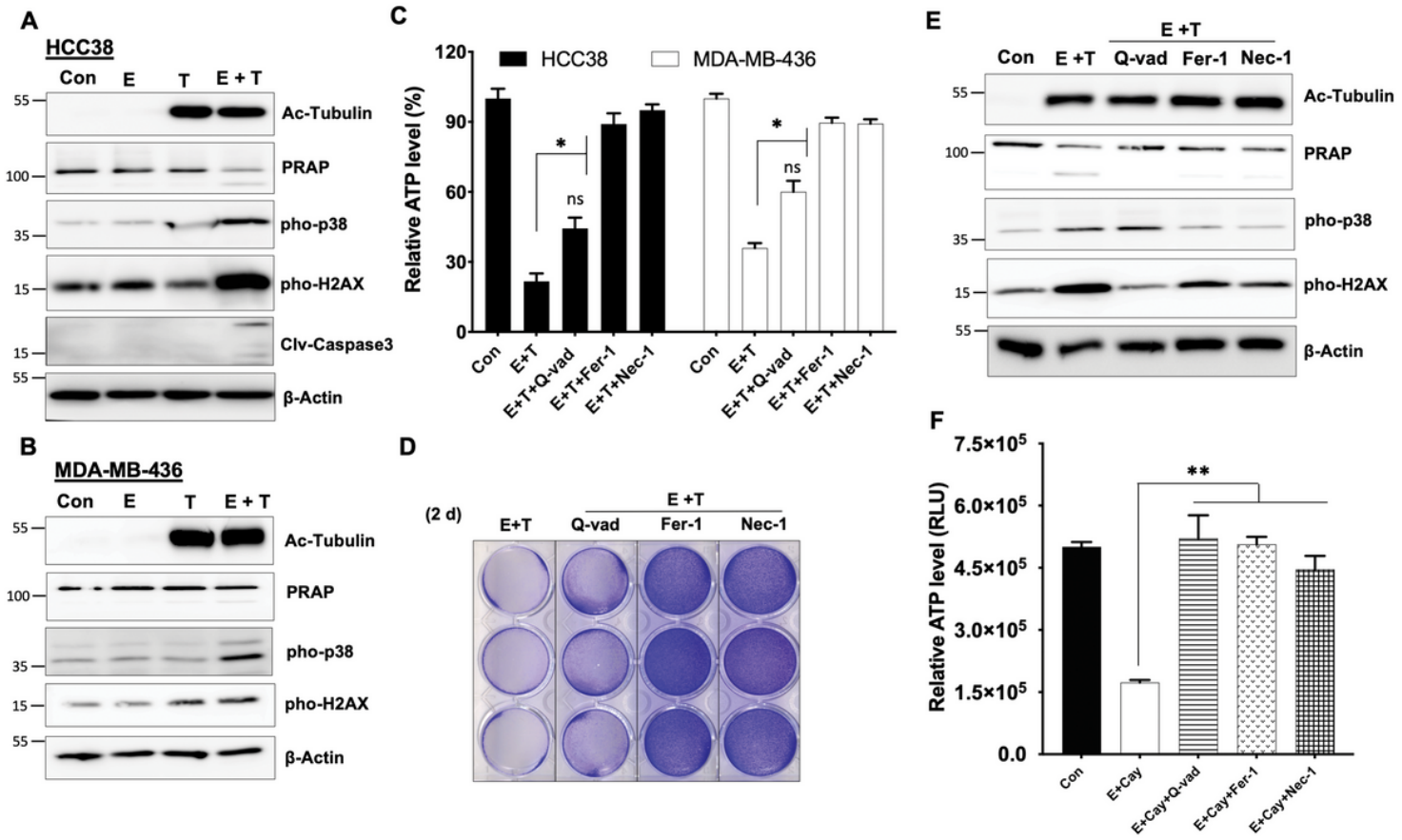

Figure 2

HDAC6 inhibitors synergize with erastin to induce a mixed type of cell death (A, B) Immunoblot analysis of acetylated-tubulin, PARP1, cleaved Caspase-3, phosphorylated p38 and H2AX protein expression in HCC38 (A; 24 hrs) and in MDA-MB-436 (B; 36 hrs) under treatments with either control (Con), 5 μM erastin (E), 5 μM tubacin (T), or combination of erastin and tubacin (E+T); β-Actin serves as a protein normalization control. (C, D) Relative cell survival of HCC38 (48hrs) and MDA-MB-436 (72hrs) were measured by CellTiter-Glo assay (C; n=3, *, $p<0.001$) or HCC38 assessed by crystal violet (D) under either Con, combination of E+T, or E+T with different cell death inhibitors Q-Vad (10 μM), Fer-1(10 μM), Nec-1 (20 μM) for 48 hours. (E) Immunoblot analysis of indicated protein expression in HCC38 cells treated as (C) for 24 hours. (F) Relative cell survival was measured by CellTiter-Glo assay in HCC38 cells treated with either control (Con), combination of erastin and 2 μM Cay (E+Cay), or E+Cay with following death inhibitors Q-Vad 10 μM, Fer-1 (10 μM; **, $p<0.005$), Nec-1 (20 μM; **, $p<0.005$) for 48 hours.

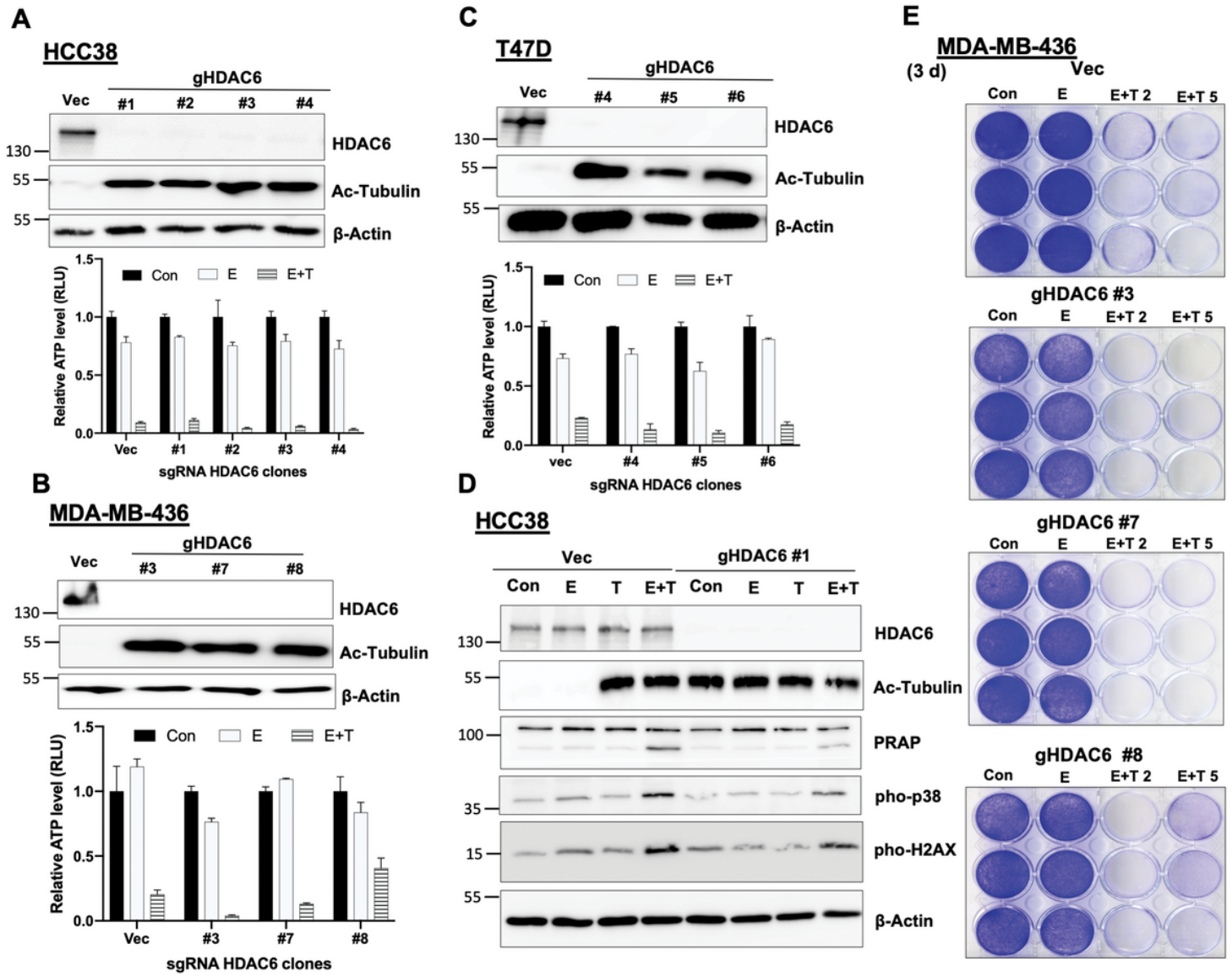

Figure 3

Knockout of HDAC6 fails to mimic tubacin to promote cell death (A, B, C) Immunoblotting analysis (Upper panel) of HDAC6 and acetylated tubulin in the empty vector (Vec) and different sgRNA targeted HDAC6 clones (gHDAC6) of HCC38 (A), MDA-MB-436 (B), and luminal T47D (C). -Actin serves as a protein normalization control. Relative cell survival (Lower panel) was measured by the ATP level in indicated cells under either control (Con), 5 μM erastin, or combination of erastin and 5 μM tubacin (E+T) for 72 hours (n=3). (D) Western blot analysis of indicted protein expression in HCC38 Vec or gHDAC6 HCC38 cells (Clone #1) treated with either control (Con), 5 μM erastin (E), 5 μM tubacin (T), or combination of erastin and tubacin (E+T) for 24 hrs. (E) Cell viability was assessed by crystal violet staining in MDA-MB-436 empty vector cells or different gHDAC6 clones under either control (Con), erastin (E), or erastin with different doses of tubacin (E+T) treatment for 72 hrs.

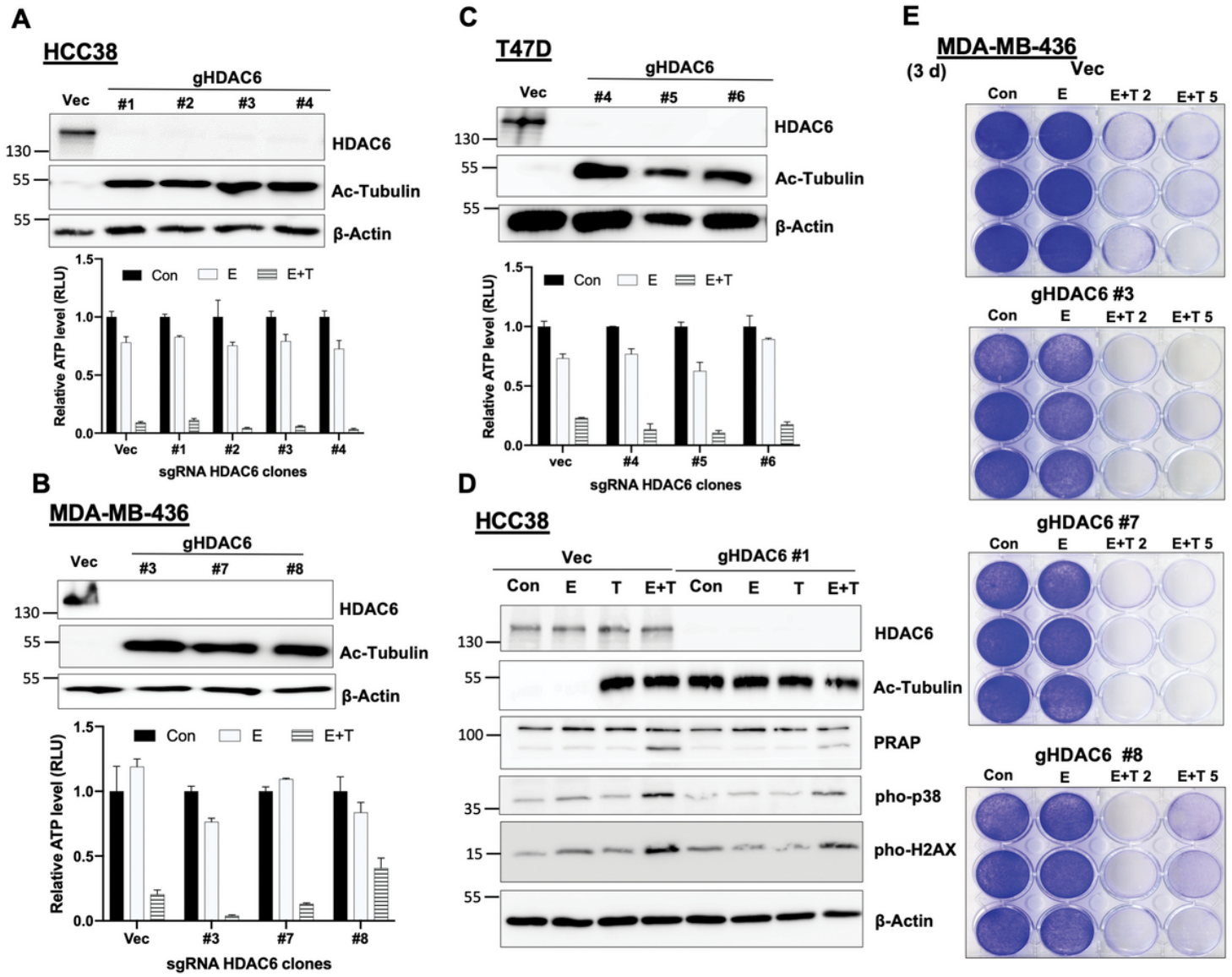

Figure 3

Knockout of HDAC6 fails to mimic tubacin to promote cell death (A, B, C) Immunoblotting analysis (Upper panel) of HDAC6 and acetylated tubulin in the empty vector (Vec) and different sgRNA targeted HDAC6 clones (gHDAC6) of HCC38 (A), MDA-MB-436 (B), and luminal T47D (C). -Actin serves as a protein normalization control. Relative cell survival (Lower panel) was measured by the ATP level in indicated cells under either control (Con), 5 μM erastin, or combination of erastin and 5 μM tubacin (E+T) for 72 hours (n=3). (D) Western blot analysis of indicted protein expression in HCC38 Vec or gHDAC6 HCC38 cells (Clone #1) treated with either control (Con), 5 μM erastin (E), 5 μM tubacin (T), or combination of erastin and tubacin (E+T) for 24 hrs. (E) Cell viability was assessed by crystal violet staining in MDA-MB-436 empty vector cells or different gHDAC6 clones under either control (Con), erastin (E), or erastin with different doses of tubacin (E+T) treatment for 72 hrs.

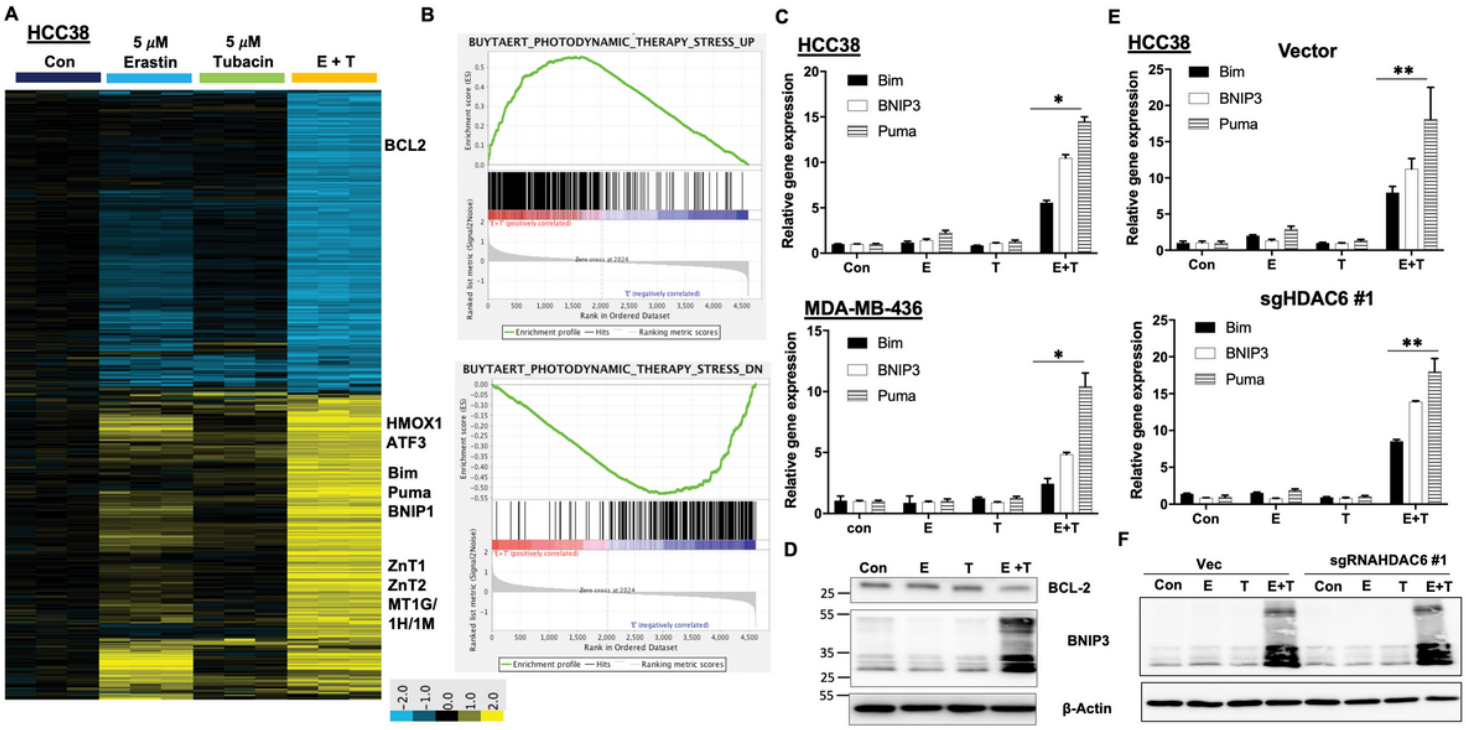

Figure 4

Tubacin synergizes with erastin to induce a distinct gene transcriptional program (A) Heatmap cluster view of transcriptional profiling in HCC38 cells under treatments of either control (Con), 5 μM erastin (E), 5 μM tubacin (T), or combination of erastin and tubacin (E+T) for 24 hrs. (B) GSEA analysis indicates gene expression profile induced by E+T are comparable to the transcriptional response of photodynamic therapy. (C, D) RT-qPCR analysis of apoptotic gene expression in HCC38 and MDA-MB-436 (n=3, *, $p<0.001$) cells under the similar treatments to (A). (D) Immunoblot analysis of BCL-2 and BNIP3 protein expression in HCC38 cells under the similar treatments to (A). (E) RT-qPCR analysis of apoptotic gene expression in HCC38 Vector and sgRNAHDAC6 #1 cells (#, $p<0.0001$) under the similar treatments to (A). (F) Immunoblot analysis of BNIP3 protein expression in HCC38 Vector (Vec) and sgRNAHDAC6 #1 cells under the similar treatments to (A).

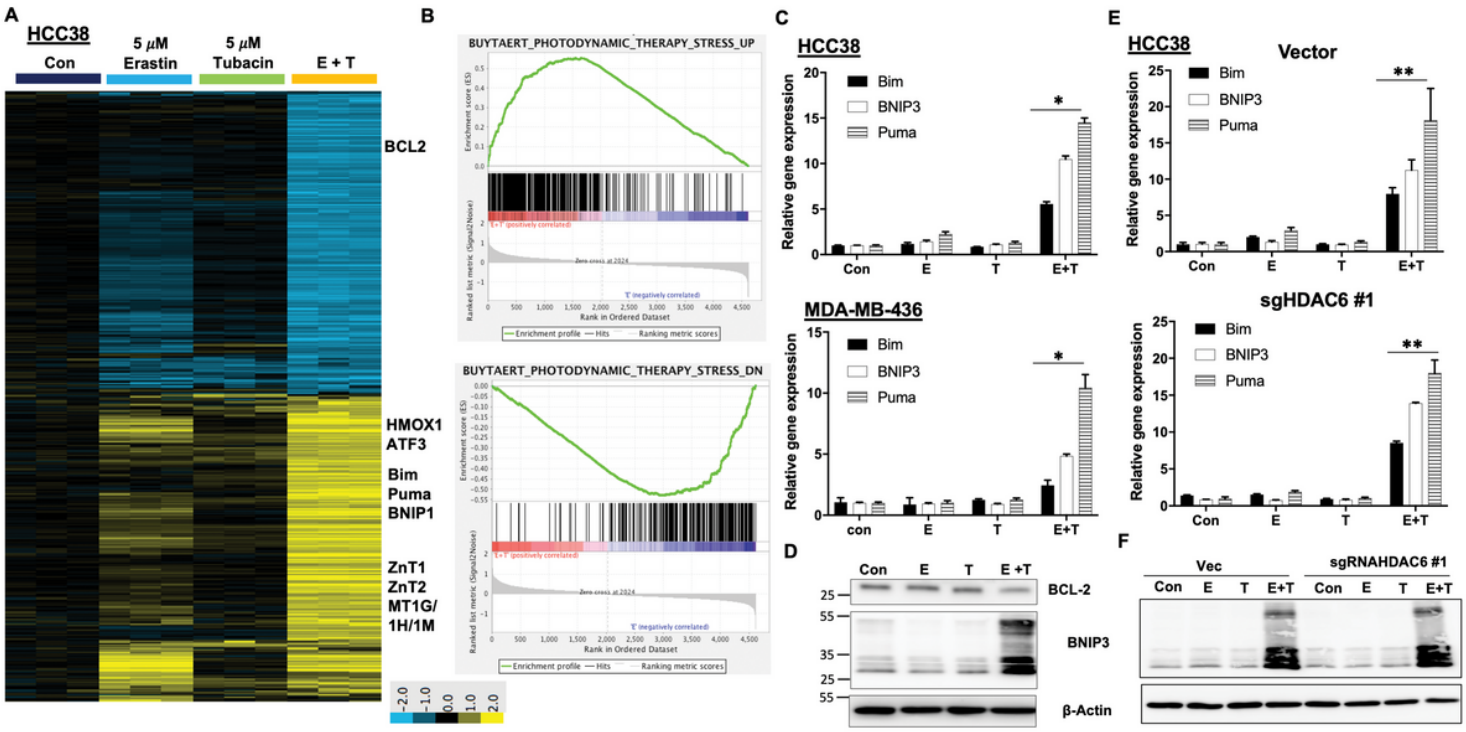

Figure 4

Tubacin synergizes with erastin to induce a distinct gene transcriptional program (A) Heatmap cluster view of transcriptional profiling in HCC38 cells under treatments of either control (Con), 5 μM erastin (E), 5 μM tubacin (T), or combination of erastin and tubacin (E+T) for 24 hrs. (B) GSEA analysis indicates gene expression profile induced by E+T are comparable to the transcriptional response of photodynamic therapy. (C, D) RT-qPCR analysis of apoptotic gene expression in HCC38 and MDA-MB-436 (n=3, *, $p<0.001$) cells under the similar treatments to (A). (D) Immunoblot analysis of BCL-2 and BNIP3 protein expression in HCC38 cells under the similar treatments to (A). (E) RT-qPCR analysis of apoptotic gene expression in HCC38 Vector and sgRNAHDAC6 #1 cells (#, $p<0.0001$) under the similar treatments to (A). (F) Immunoblot analysis of BNIP3 protein expression in HCC38 Vector (Vec) and sgRNAHDAC6 #1 cells under the similar treatments to (A).

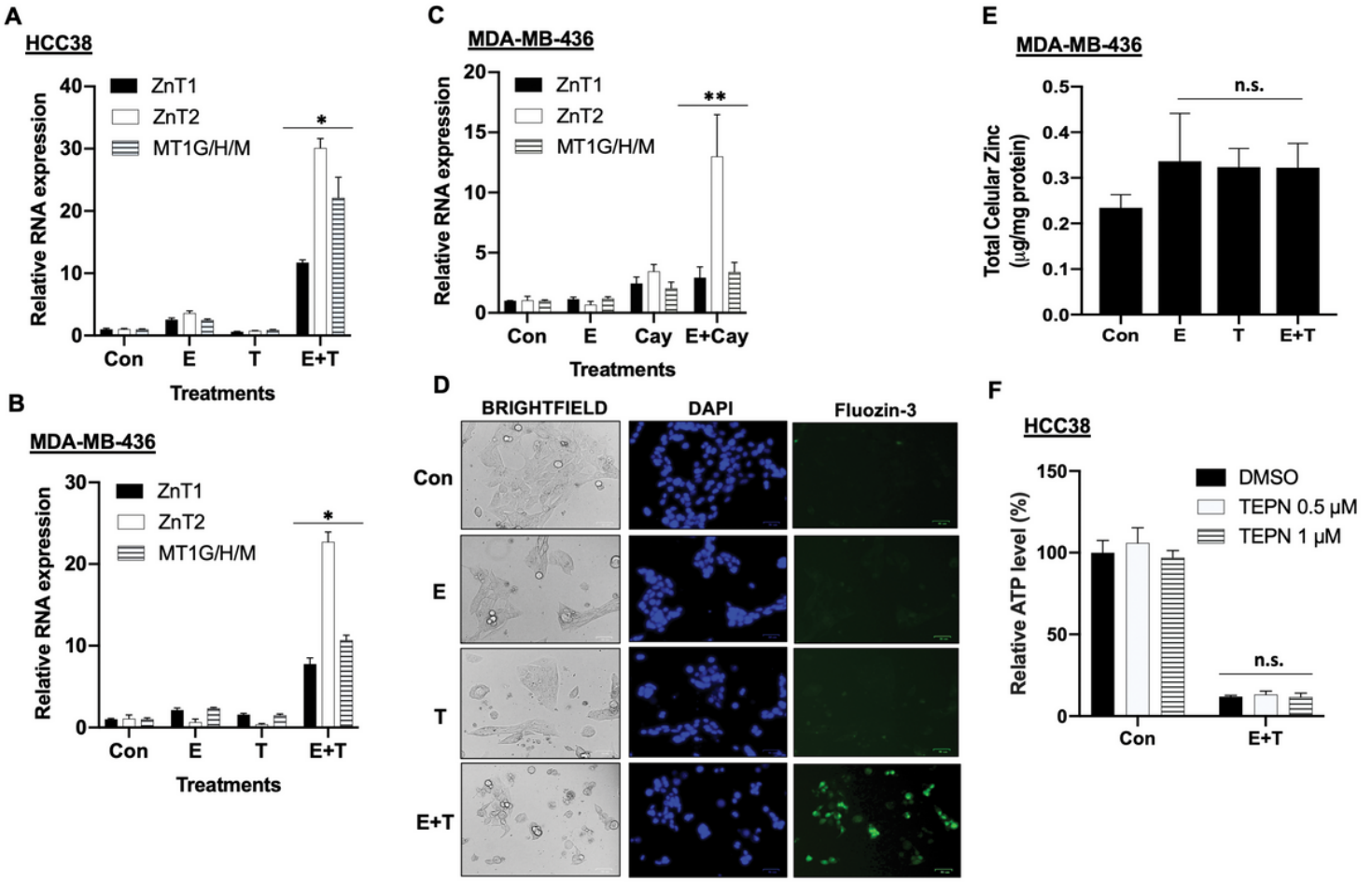

Figure 5

The zinc-related gene response is triggered by erastin with tubacin (A, B) RT-qPCR expression analysis of genes involved in zinc homeostasis (n=3, *, p<0.005) in HCC38 cells (A; 24 hrs) and MDA-MB-436 (B; 36 hrs) under treatments of either control (Con), 5 μM erastin (E), 5 μM tubacin (T), or combination of erastin and tubacin (E+T). (C) RT-qPCR expression analysis of genes involved in zinc homeostasis (n=3, **, p<0.005) in MDA-MB-436 (36 hrs) under treatments of either control (Con), 5 μM erastin (E), 5 μM Cay10603 (Cay), or combination of erastin and Cay10603 (E+Cay). (D) Living cell imaging of HCC38 cells was stained by Fluozin-3 and DAPI (Hoechst 33342) under the similar treatments to (A) for 18 hrs. The size of scale bar is 100 μM. (E) Total cellular zinc was measured by ICP-AES analysis (n=3, n.s., not significant) in MDA-MB-436 cells under either control (Con), 5 μM erastin (E), 5 μM tubacin (T), or combination of erastin and tubacin (E+T) for 24 hours. (F) Relative cell viability of HCC38 cells was measured by the ATP level under either control or E+T treatment with addition of different concentration of TPEN for 48hrs (n=3, n.s., not significant).

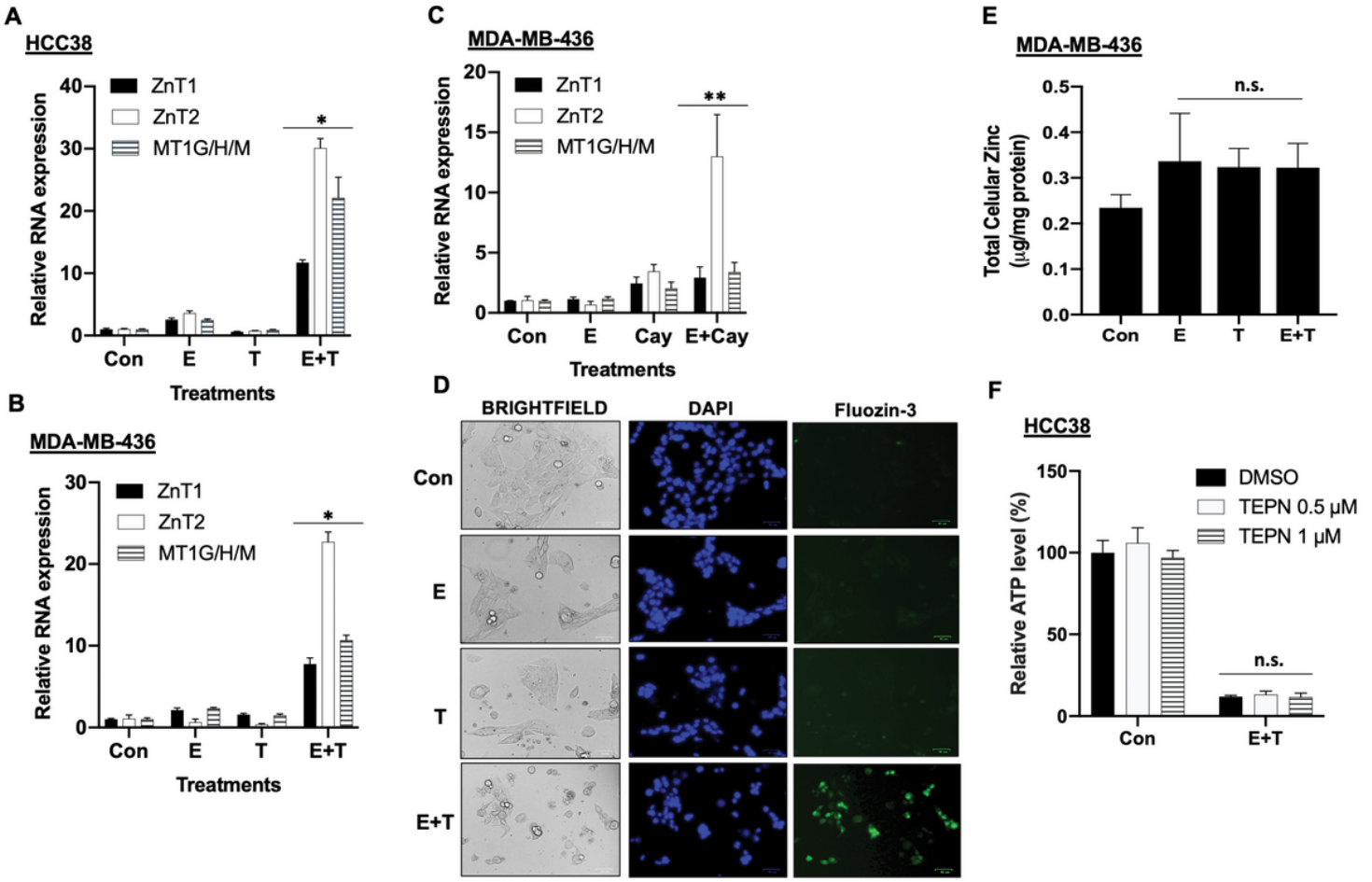

Figure 5

The zinc-related gene response is triggered by erastin with tubacin (A, B) RT-qPCR expression analysis of genes involved in zinc homeostasis (n=3, *, p<0.005) in HCC38 cells (A; 24 hrs) and MDA-MB-436 (B; 36 hrs) under treatments of either control (Con), 5 μM erastin (E), 5 μM tubacin (T), or combination of erastin and tubacin (E+T). (C) RT-qPCR expression analysis of genes involved in zinc homeostasis (n=3, **, p<0.005) in MDA-MB-436 (36 hrs) under treatments of either control (Con), 5 μM erastin (E), 5 μM Cay10603 (Cay), or combination of erastin and Cay10603 (E+Cay). (D) Living cell imaging of HCC38 cells was stained by Fluozin-3 and DAPI (Hoechst 33342) under the similar treatments to (A) for 18 hrs. The size of scale bar is 100 μM. (E) Total cellular zinc was measured by ICP-AES analysis (n=3, n.s., not significant) in MDA-MB-436 cells under either control (Con), 5 μM erastin (E), 5 μM tubacin (T), or combination of erastin and tubacin (E+T) for 24 hours. (F) Relative cell viability of HCC38 cells was measured by the ATP level under either control or E+T treatment with addition of different concentration of TPEN for 48hrs (n=3, n.s., not significant).

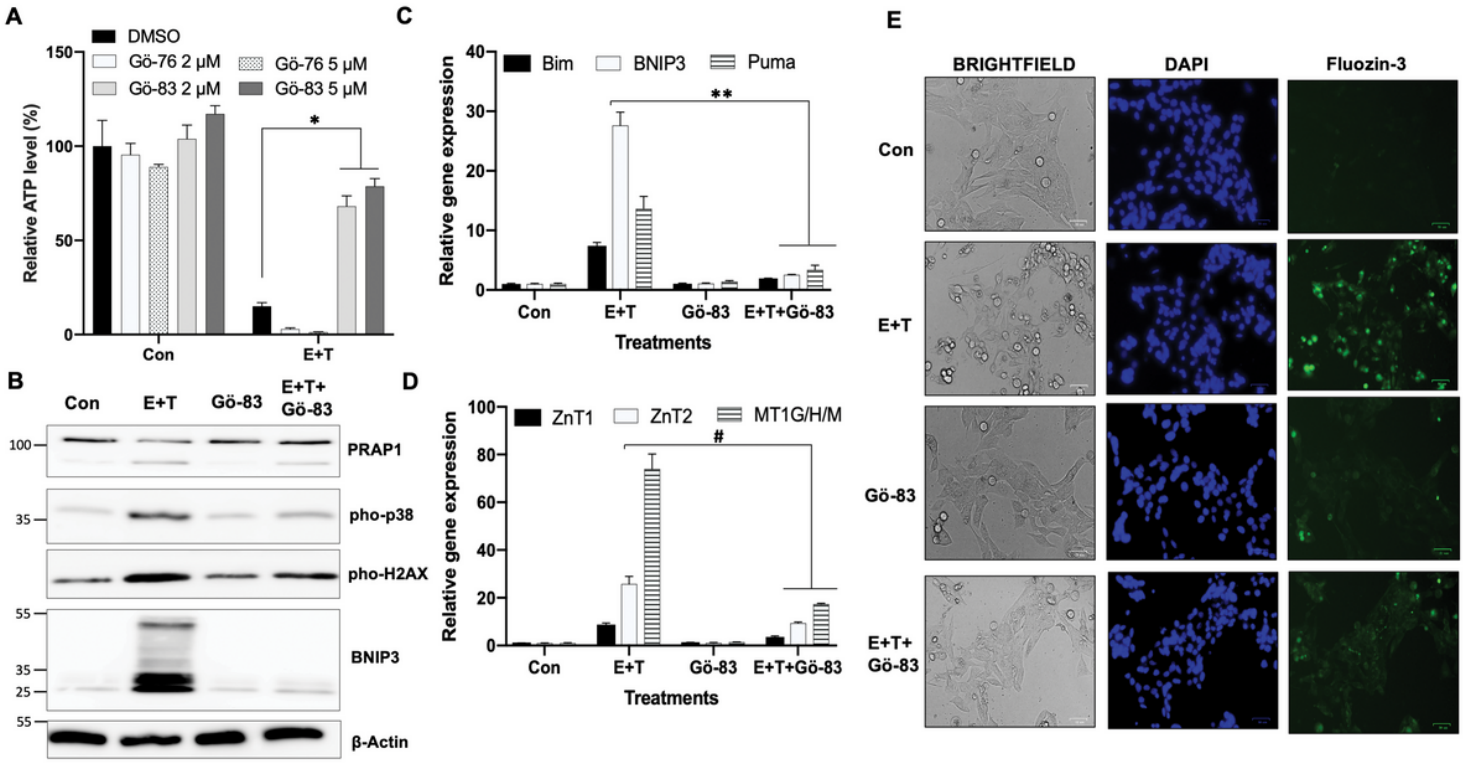

Figure 6

PKC activation is required for the increase of labile zinc and cell death (A) Relative cell survival was measured by relative ATP level in HCC38 cells under either control or 5 μM erastin and 5 μM tubacin (E+T) treatment with or without addition of different doses of PKC inhibitor Gö 6976 or Gö 6983 for 72 hrs (n=3, *, $p<0.005$). (B) Western blot analysis of indicted protein expression in HCC38 cells under similar treatments to (A) for 24 hrs. (C, D) RT-qPCR expression analysis of indicated apoptotic genes (C; **, $p<0.001$) and zinc-related genes (D; #, $p<0.0001$) under similar treatments to (B). (E) Living cell imaging of HCC38 cells was stained by Fluozin-3 and DAPI (Hoechst 33342) under the similar treatments to (B) for 18 hrs. The size of scale bar is 50 μm.

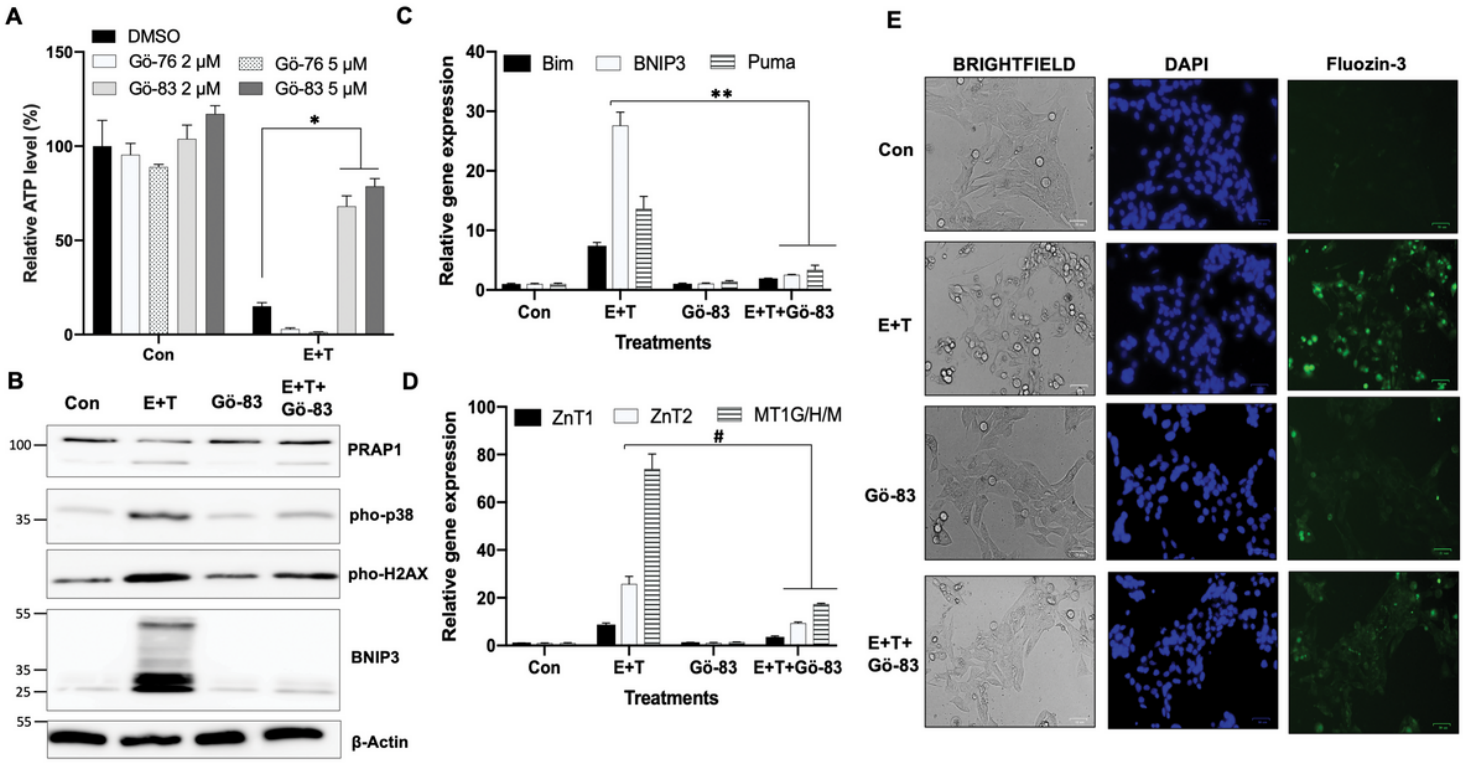

Figure 6

PKC activation is required for the increase of labile zinc and cell death (A) Relative cell survival was measured by relative ATP level in HCC38 cells under either control or 5 μM erastin and 5 μM tubacin (E+T) treatment with or without addition of different doses of PKC inhibitor Gö 6976 or Gö 6983 for 72 hrs (n=3, *, $p<0.005$). (B) Western blot analysis of indicted protein expression in HCC38 cells under similar treatments to (A) for 24 hrs. (C, D) RT-qPCR expression analysis of indicated apoptotic genes (C; **, $p<0.001$) and zinc-related genes (D; #, $p<0.0001$) under similar treatments to (B). (E) Living cell imaging of HCC38 cells was stained by Fluozin-3 and DAPI (Hoechst 33342) under the similar treatments to (B) for 18 hrs. The size of scale bar is 50 μm.

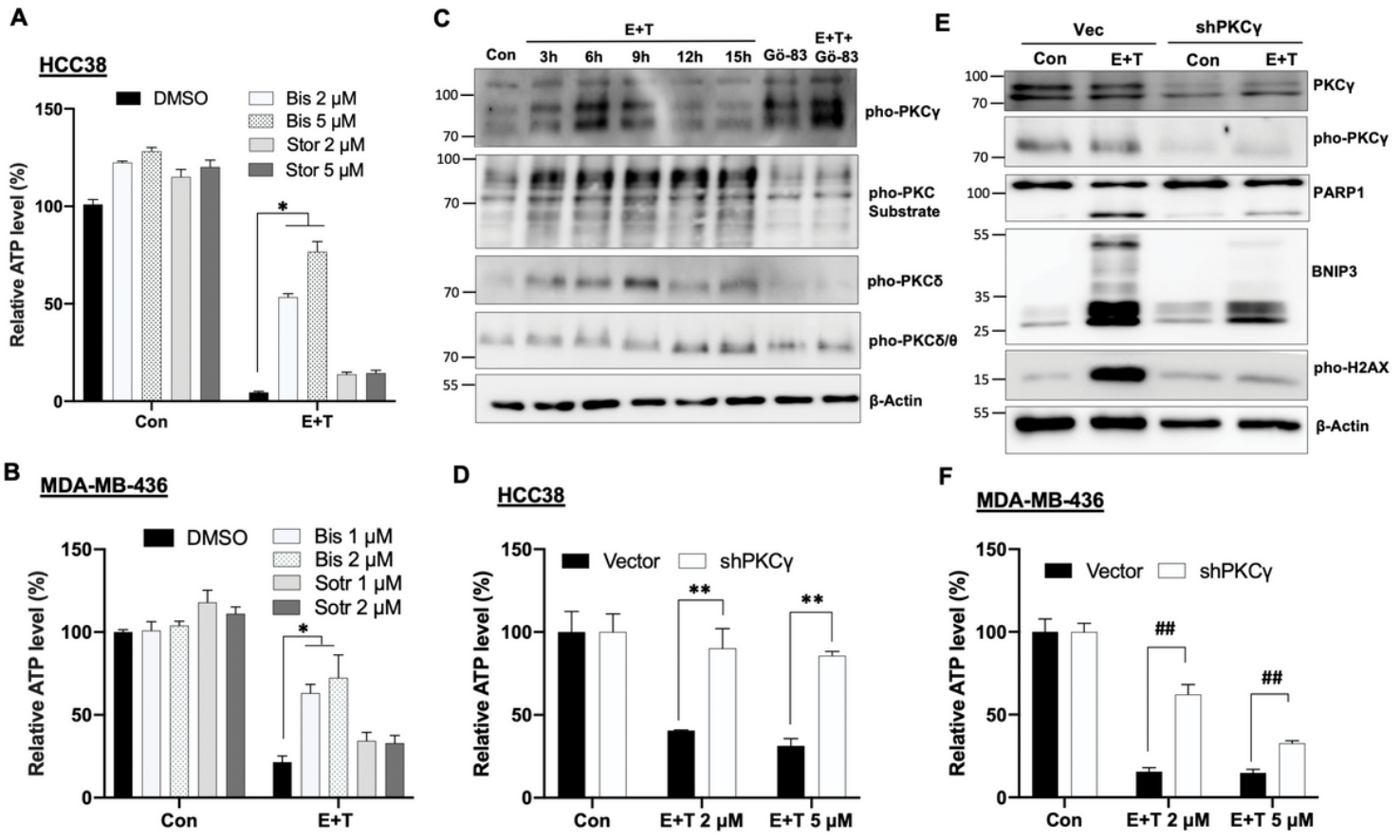

Figure 7

PKCγ is required for the tubacin-promoting cell death (A, B) Relative cell survival was measured by the ATP level in HCC38 and (B) MDA-MB-436 under either control (Con) or 5 μM erastin and 5 μM tubacin (E+T) treatment with or without addition of different doses of PKC inhibitors bisindolylmaleimidel (Bis) or sotrastaurin (Sotr) for 72 hrs (A, n=3, *, p<0.001)(B, n=3, *, p<0.005). (C) Western blot analysis of indicated proteins expression in MDA-MB-436 cells under the control and E+T treatments with or without Gö 6983 for indicated times. (D) Cell viability was measured by the relative ATP level of HCC38 Vec and shPKCγ cells under either Con, or 5 μM erastin with different doses of tubacin for 48 hrs (n=4, **, p<0.01). (E) Immunoblotting analysis of indicated protein expression in HCC38 with vector and shPKCγ cells under either Con, or erastin plus tubacin for 24 hrs. (F) Cell viability was measured by the relative ATP level of MDA-MB-436 Vec and shPKCγ cells under either Con, or 5 μM erastin with different doses of tubacin for 72 hrs (n=4, ## p<0.01).

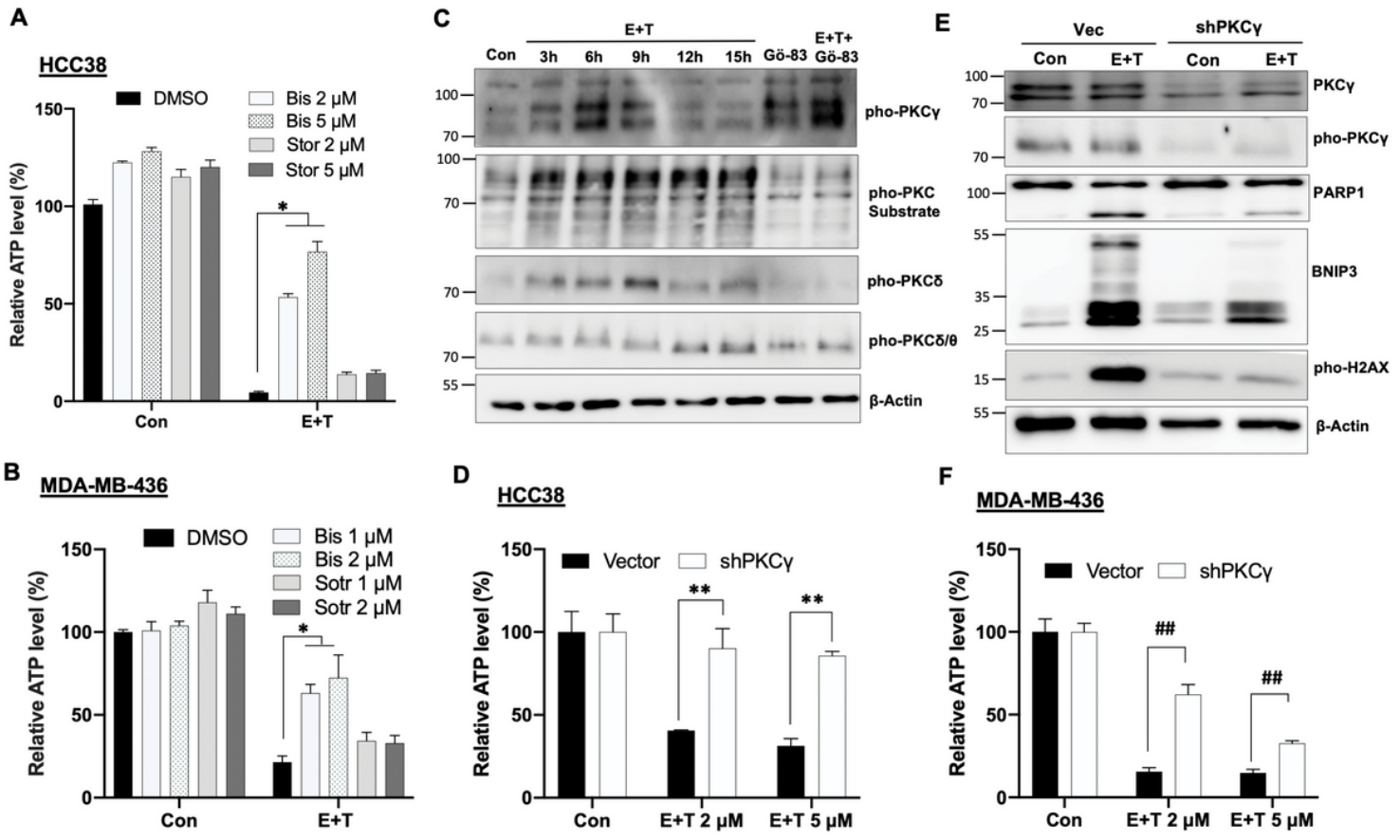

Figure 7

PKCγ is required for the tubacin-promoting cell death (A, B) Relative cell survival was measured by the ATP level in HCC38 and (B) MDA-MB-436 under either control (Con) or 5 μM erastin and 5 μM tubacin (E+T) treatment with or without addition of different doses of PKC inhibitors bisindolylmaleimidel (Bis) or sotrastaurin (Sotr) for 72 hrs (A, n=3, *, p<0.001)(B, n=3, *, p<0.005). (C) Western blot analysis of indicated proteins expression in MDA-MB-436 cells under the control and E+T treatments with or without Gö 6983 for indicated times. (D) Cell viability was measured by the relative ATP level of HCC38 Vec and shPKCγ cells under either Con, or 5 μM erastin with different doses of tubacin for 48 hrs (n=4, **, p<0.01). (E) Immunoblotting analysis of indicated protein expression in HCC38 with vector and shPKCγ cells under either Con, or erastin plus tubacin for 24 hrs. (F) Cell viability was measured by the relative ATP level of MDA-MB-436 Vec and shPKCγ cells under either Con, or 5 μM erastin with different doses of tubacin for 72 hrs (n=4, ## p<0.01).

Supplementary Files

This is a list of supplementary files associated with this preprint. Click to download.

- SupplementalTable1.xlsx
- SupplementalTable1.xlsx

- SupplementalTable2.xlsx
- SupplementalTable2.xlsx
- SupplementaryFigureLegends11062020.pdf
- SupplementaryFigureLegends11062020.pdf
- SupplementaryFigures11062020.pdf
- SupplementaryFigures11062020.pdf